Spring 2003

# Design and fabrication of a novel linear oscillating conventional micro air pump

Shi-Je Wu

# DESIGN AND FABRICATION OF A NOVEL LINEAR OSCILLATING CONVENTIONAL MICRO AIR PUMP

By
Shi-Je Wu, B.S. M.S.

A Dissertation Presented in Partial Fulfillment
Of the Requirement for
Degree Ph.D. in Engineering

COLLEGE OF ENGINEERING AND SCIENCE
LOUISIANA TECH UNIVERSITY

May 2003

LOUISIANA TECH UNIVERSITY

**THE GRADUATE SCHOOL**

Feb 14, 2003
Date

We hereby recommend that the thesis prepared under our supervision by Shi-Je Wu

entitled Design And Fabrication of A Novel Linear Oscillating Conventional Micro Air Pump

be accepted in partial fulfillment of the requirements for the Degree of Ph.D. in Engineering

Supervisor of Thesis Research

Head of Department

Department

Recommendation concurred in:

Advisory Committee

Approved:
Director of Graduate Studies

Approved:
Dean of the Graduate School

Dean of the College

GS Form 13
(1/00)

*To My Family,*
*Without you, I Mean Nothing.*

# ABSTRACT

A novel permanent magnetically and electro-magnetically powered, linear oscillating conventional micro air pump was designed, fabricated and characterized. This new pump might be used in a wrist-type blood pressure monitor or other similar devices that require high air pressure discharge. Factors considered in designing this micro air pump include feature size (especially the thickness), operation voltage, efficiency, heat transfer, noise and weight. For evaluating the feasibility of this novel design, basic performance calculations and ANSYS magnetic flux simulations had been conducted before the first prototype was made. Both theoretical calculations and simulation results show that this novel design meets the requirements for use in a wrist-type blood pressure monitor. The developed pump prototype pump was able to achieve a maximum air pressure of 180 mmHg.

Compared to an existing air pump used in a wrist-type blood pressure meter, this new design shows significant reduction in the thickness (reduced by 33%) as well as in the overall size (reduced by 50%). It is also quieter, environmentally friendly, and easily manufactured at low cost.

## APPROVAL FOR SCHOLARLY DISSEMINATION

The author grants to the Prescott Memorial Library of Louisiana Tech University the right to reproduce, by appropriate methods, upon request, any or all portions of this Dissertation. It is understood that "proper request" consists of the agreement, on the part of the requesting party, that said reproduction is for his personal use and that subsequent reproduction will not occur without written approval of the author of this Dissertation. Further, any portions of the Dissertation used in books, papers, and other works must be appropriately referenced to this Dissertation.

Finally, the author of this Dissertation reserves the right to publish freely, in the literature, at any time, any or all portions of this Dissertation.

Author Shi-Je Wu

Date May 22, 2003

GS Form 14
(5/03)

# TABLE OF CONTENTS

# LIST OF TABLES

# LIST OF FIGURES

Page

# ACKNOWLEDGEMENTS

There are several important contributors that help me to complete this dissertation. I would like to take this opportunity to express my sincere gratitude and appreciation to Dr. Jun-Ing Ker, Chairman of my Advisory Committee, for his guidance, advice and encouragement. I also appreciate to my advisory committee, Dr. Mickey Cox, Dr. David E. Hall, Dr. B.J. Kim and Dr. Walter Grant Besio for their guidance and support.

Many thanks are also extended to Mr. Frank Tsai at PIDC, Taiwan and Mr. Jimmy Cook for their time and expertise.

# CHAPTER 1

# INTRODUCTION

Brain hemorrhage is a key cause for human death, especially in the last 3 or 4 decades. Many researchers have devoted their time and efforts trying to find ways to control brain hemorrhage but have yet to be successful. Nevertheless, research has concluded that an increase in blood pressure would very likely increase the chance of getting brain hemorrhage.

## 1.1. Blood Pressure Monitor

The wrist-type blood pressure monitor is a handy device that can be carried easily to monitor blood pressure change. The wrist-type blood pressure monitor is not a new product; however, the trend is to make it smaller and lighter.

The miniaturization of blood pressure meters has been an on-going effort for many years. Today, there are many kinds of wrist-type blood pressure monitors that can be purchased off-the-shelf. Examples include Rossmax RM-4000, Omron HEM-609, Panasonic EW280W, Sony SDM-S71 and etc. Nevertheless, these blood pressure monitors are still too large and too heavy to be worn on the wrist at all times.

The core component for the automatic wrist blood pressure monitor is a micro pump, which is also the most difficult component to miniaturize. The traditional blood pressure monitor uses a small pump driven by a small rotary motor. Such motor has little

potential to be further reduced in its size because it is constructed by several mechanical components. As a consequence, the design of a new micro air pump, using a different approach, has recently gained great attention among blood pressure manufacturers.

Research on conventional micro pumps, however, has not often been reported, mainly because they are considered a very mature technology. Most of the conventional micro pumps adopt a rotary motor to drive a piston for air pumping. Nevertheless, a rotary motor has two major disadvantages: (1) large size, and (2) loud noise (generated from the motor brush). In recent years, improvements have been made towards reducing the size of rotary pump (by increasing the magnetic flux strength of the permanent magnet used) and decreasing its noise (by adopting a brushless design). Unfortunately, the small compartment of many miniaturized devices being developed does not provide ample space to accommodate a rotary motor.

The oscillating motor/driver and the linear motor/driver are alternatives to the rotary motor and have a better potential to meet the needs of many miniaturized pumps being developed today. Compared to the rotary motor, linear and oscillating motor/driver show lots of advantages in small size applications, such as simple design, efficiency, frequency control, quiet, small size, less maintenance and reliability compared to their rotary competitor. Examples of practical applications include speakers and compression drivers, active noise and vibration control, sonar and ultrasonic, vibratory processing equipments and acoustic compressors [01]. Driving of an oscillating motor/driver involves two forces – electromagnetic and/or mechanical spring force. Thus, its power (pumping capacity or volume) is often limited by the small stroke distance of the piston, and its

operation is more complicated. As a result, care must be taken in designing an oscillating motor to be used in a miniaturized pump.

## 1.2 Research Objective

The objective of this study is to present the design, fabrication and characterization of a novel conventional micro pump by using linear and oscillating motor/driver concepts. It is the intent of the author to develop a smaller micro air pump that could be used on wrist blood pressure monitor or other applications. Unlike the traditional oscillating motor/driver using just one driving magnetic force (either attractive or repulsive) or a combination force of magnetic force and mechanical spring force to drive the piston, the proposed new micro air pump will be developed based on a new double driving magnetic forces concept. (Both attractive and repulsive forces are applied simultaneously).

## 1.3 Organization of Dissertation

This dissertation is organized into six Chapters. Chapter 1 Introduction; Chapter 2 Theory, literature review, and survey of current conventional micro pumps; Chapter 3 Design, operation principle, performance calculation and simulation; Chapter 4 Design review and fabrication; Chapter 5 Final assembly, experiment setups and results analysis and Chapter 6 Conclusions and recommendations for the future research.

# CHAPTER 2

# THEORY, LITERATURE REVIEW AND SURVEY OF CURRENT CONVENTIONAL MICRO PUMPS

The concepts related to this study will include pumping processes (pump, reciprocating pump), magnetism (basic theories of permanent magnets and electromagnets, brushless motors, linear motors, electromagnetic actuators and etc.), digital oscillating drivers (digital oscillating control circuits), and blood pressure monitors. In this chapter, these concepts, devices, and related research will be briefly discussed. In addition, some conventional micro pumps available on today's market will be reviewed.

## 2.1 Pumps

Pumps - machines that add energy to fluids - are the oldest known devices to transfer fluid in human history [01]. Almost 3000 years ago, undershoot-bucket waterwheels were used in Asia and Africa, and they are still common today. Another early example is Archimedes' screw pump (around 250 BC), still being manufactured to

handle solid-liquid mixtures [02]. Pumps have been widely used in our daily life, from the power plant to the coffee maker; from chemical laboratory to the artificial heart; from the space shuttle's main hydrogen-oxygen engine to car's fuel injection system, etc. Pumps remain probably the second most common machine in use, exceeded in numbers only by the electric motor [03]. In general, depending on how the energy is added into the fluid, pumps may be divided into two major types: (a) dynamic pumps and (b) positive displacement pumps.

Dynamic pumps (Centrifugal pumps) include volute pumps, turbine pumps, axial pumps and mixed flow pumps. One example of a dynamic pump is shown in Figure 2.1a [04], in which energy is continuously added by means of fast-moving blades or vanes or certain special designs to increase the fluid [02]. There is no closed volume in this design; the fluid momentum increases while moving through open passages and then converts its high velocity into a pressure increase by exiting into a diffuser section [03].

Positive displacement pumps (Reciprocating or Rotary pumps) include piston pumps, plunger pumps, diaphragm pumps, gear pumps, screw pumps, vane pumps and etc. One such example is shown in Figure 2.1b [04], in which energy is periodically added by application of force to one or more movable boundaries of any desired number of enclosed, fluid containing volumes, resulting in a direct increase in pressure up to the value required to move the fluid through valves or ports into the discharge line [03]. There is a constant volume for each pumping.

To sum up, dynamic pumps are more suitable for a higher flow rate, a steadier discharge, and lower viscosity liquids applications than positive displacement pumps are.

On the other hand, positive displacement pumps are appropriate for high-pressure rise and low flow rate, while dynamic pumps provide a high flow rate with low-pressure rise.

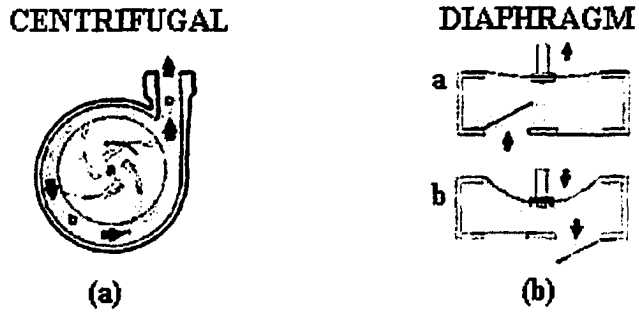


**Figure 2.1 Example of the two different types of pumps, (a) Dynamic pump; (b) Positive displacement pump [4]**

### 2.1.1 Reciprocating Piston Pump

The reciprocating pump design (as seen in Figure 2.2) is widely used for high-suction head and low-volume pumping system. Traditionally, there are two types of reciprocating pumps – direct-acting steam-driving units and power pumps. The power for the reciprocating pump is a steam engine or motor (the electro motor driver will be the major type discussed here.) With the aid of steam or an electro motor to drive the piston to do reciprocating actions, the pump will transfer the gas/liquid intermittently. The basic operation steps of the reciprocating pump are: (Also shown in Figure 2.2)

1. The motor will keep running and by the shifts; it will change the piston direction to keep the piston moving up and down.

2. The pressure difference caused by the piston will make the inlet/outlet valves open and close to finish a pumping cycle.

The average capacity of the reciprocating pump could be gotten by the following equation, Eq.2.1

$$Q = \eta_v * j * A * S_p * n/60 \qquad (2.1)$$

Here

**Q:** the average pumping volume ($mm^3$)

**$\eta_v$:** volume efficiency (for a large pump 0.97~0.99; for a small pump 0.85~0.90.)

**j:** the number of cylinders/pistons

**A:** the cylinder/piston cross-section area ($mm^2$)

**$S_p$:** stroke distance (mm)

**n:** frequency (rpm)

There are two major drawbacks in this design: there will be some energy loss during the power/direction transfer and, since this system combines two parts-pump and motor, its feature size could be too large for some special applications.

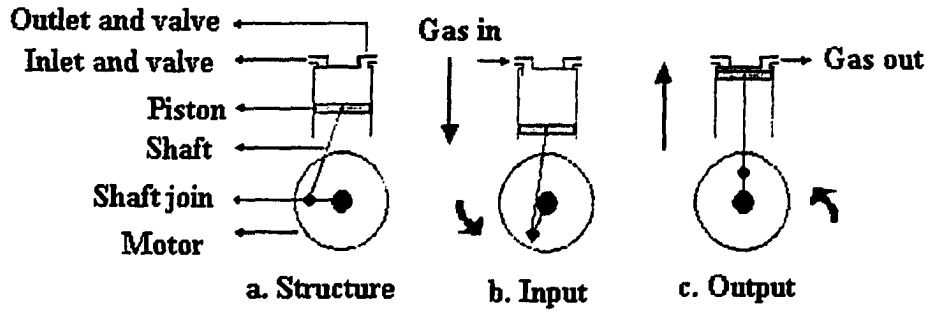


**Figure 2.2 Structure of reciprocating pump and pumping processes**

## 2.2 Magnetism

The phenomenon of magnetism was known to the Greeks as early as 800 B.C. and, perhaps even earlier to the Chinese (compass, 2500 B.C). Today, the generation of the magnetic fields could be divided into two different sources – permanent magnets and electromagnets. Every magnet (either permanent magnet or electromagnet), regardless its shape, will always have two poles, called north and south poles. Just as electric charges will exert forces on each other, the like magnetic poles will repel each other, and the unlike magnetic poles will attract each other (as shown in Figure 2.3). Although the force interactions between two magnetic poles are similar to what happens between two electric charges, there is an important difference. The electric charges can be isolated (as in the case of the electron and proton), but magnetic poles cannot. That is, they are always found in pairs [05]. All attempts tried to detect an isolated magnetic monopole have never been successful.

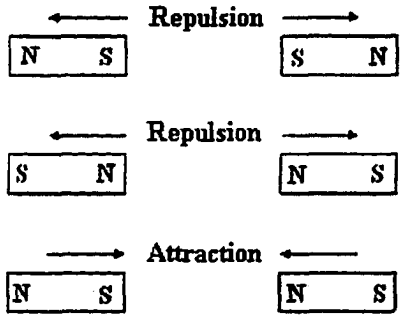


**Figure 2.3 Three possible reactions between two different magnetic poles**

### 2.2.1 General Magnetic Theories

In 1819, the Danish scientist Hans Oersted discovered the relationship between magnetism and electricity. After that, many basic theories have been discovered and built, such as the Lorentz force law, Biot-Savart's law, Ampere's law and etc. To complete the basic understanding about the magnetism, some important theories will be discussed in the following paragraphs.

**Lorentz Force Law.** Lorentz force law is the basic operation concept for all magnetic field machine applications that convert electrical energy to mechanical energy. If a straight conductor of length l meters carries a current of i amperes and is situated in a uniform magnetic field of density B Tesla, the Lorentz force exerted on the conductor is (Eq.2.2 in vector form) [05][06][07]

$$\vec{F} = l\,\vec{i} \times \vec{B} \tag{2.2}$$

The implications of this expression include:

1. The force is perpendicular to both the direction of the current i and the magnetic field B.
2. The direction of the force is given by the right hand rule. The force relationship above is in the form of a vector product. (See Figure 2.4.)

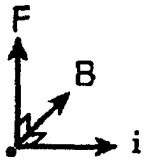


**i, direction of the current**

**Figure 2.4. Directions of magnetic force, current and magnetic field**

**Biot-Savart's Law.** Biot-Savart's Law says that if a wire carries a steady current i, at the point ***P*** associated with the element ***ds***, the wire will generate a magnetic field ***dB*** (see Eq.2.3),

$$dB = \frac{\mu_0}{4\cdot\pi}\frac{ids\cdot\hat{r}}{r^2} \tag{2.3}$$

Here

dB: the total magnetic field generated by the current

$\mu_0$: the permeability of free space ($4\pi*10^{-7}$ Wb/A·m)

i: the current (in amperes)

r: the distance between the wire and the working point (in meters)

$\hat{r}$: the unit vector (directed from the element to the working point)

ds: element

There is one thing that needs to be noted; Biot-Savart's Law can only point out the magnetic field at a small element of the conductor. That means, to get the total magnetic field ***B*** generated by the conductor, an integration must be done (see Eq.2.4).

$$B = \frac{\mu_0 \cdot i}{4 \cdot \pi} \int \frac{\hat{r}\, ds}{r^2} \tag{2.4}$$

**Ampere's Law.** Basically, Ampere's Law is calculated for the special case of a circular path surrounding a wire; however, the result could be applied to a general case in which an arbitrary closed path is threaded by a steady current. That is, Ampere's Law says that the linear integral of **B**ds around any closed path equals $\mu_0$ i, where i is the total steady current threaded by the path (see Eq.2.5) (Ampere's Law is valid only for steady current and magnetic field configurations with a high degree of symmetry).

$$\int \mathbf{B}\ \mathbf{ds} = \mu_0 \cdot i \tag{2.5}$$

**Magnetic field of a solenoid.** A solenoid (see Figure 2.5) is a long wire wound in the form of a helix [05]. With this configuration, one can produce a reasonably uniform magnetic field within a small volume of the solenoid's interior region if the consecutive turns are closely spaced. That is, if each turn is close enough, each turn can be regarded

as a circular loop, and the total magnetic flux is the vector sum of the fluxes due to all the turns. Based on Ampere's Law, if N is the number of turns in the length l, then the total current through the solenoid is Ni, thus, Eq.2.6

$$\int \mathbf{B}\,\mathbf{ds} = Bl = \mu_0 N i$$

$$\int \mathbf{B}\,\mathbf{ds} = Bl = \mu_0 n i \qquad (2.6)$$

Here

n=N/l is the number of turns per unit length.

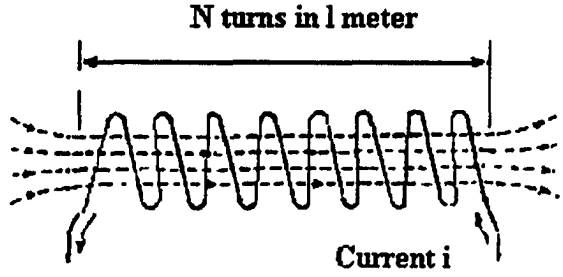


**Figure 2.5 Solenoid**

**Force of magnetic field.** Most permanent magnets are designed to provide a magnetic field to interact with some other electromagnets (coils) to get the actions that are expected, such as the motor or generator effect. However, permanent magnets are also used for their ability to attract and hold ferromagnetic objects and their ability to attract and repel some other permanent magnets.

To get the magnetic force equation, consider the following setup: a ferromagnetic pole surface, say soft iron, (cross-section area is A) is placed at at distance *l* (air gap) from another permanent magnet pole surface ($B_r$ the magnetic field strength). Thus, the energy stored in the air gap is

$$E = \frac{(B_r)^2 \times l \times A \times 10^{-8}}{0.8\pi} \quad \text{Joules} \tag{2.7}$$

If some force is added to cause the ferromagnetic to move forward or away directly to the permanent magnet pole surface a distance *l*, the energy gain (close) or loss (away) dE, can be expressed as

$$dE = F \cdot dl \quad \text{or} \quad F = \frac{dE}{dl} \tag{2.8}$$

F is the force that exerted or produced by the system. Combining Eq.2.7 and Eq.2.8, the force equation can be expressed as Eq.2.9. Here F is in dynes, $B_r$ is in gauss and A is in $cm^2$.

$$F = \frac{B_r^2 \times A}{8\pi} \tag{2.9}$$

### 2.2.2 Related Magnetic Applications

**Linear Motor.** If a rotary motor is split radially along its axis of rotation and flattened out, then what was the stator is now a forcer and the rotor becomes a coil or magnet rail (see Figure 2.6). The linear motor will produce direct linear force instead of torque. For convenience, the rotor is assumed to be solid iron. In the conventional machine, the rotor moves. In the linear motor, the long rotor can be a stationary track and the short stator can move [10].

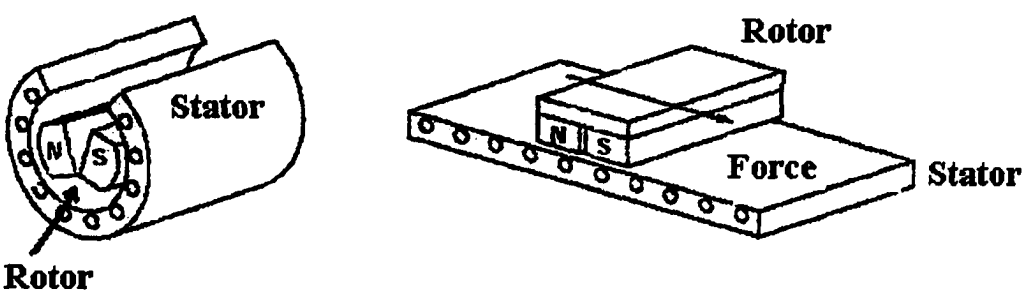


**Figure 2.6 Concepts of the linear motor [10]**

**Brushless Motor.** The major disadvantage of the brush DC motor is that it needs a commutator. The commutators and brushes wear during the operation; this will cause more maintenance. To solve this problem, the brushless motor was created. This motor has its armature winding on the stator and the field system on the rotor [11].

The function of the commutators on a conventional DC motor is to maintain an armature mmf axis always at right angles to the pole axis, regardless of the rotor position. To replace the commutators' function, an electronic sensor-switching circuit must be installed for brushless motors to keep the armature always ahead of the field of the rotor

poles. Figure 2.7 shows a diagram of the main elements of the brushless DC motor and how it works. When the armature isn't powered (Figure 2.7a), the armature will stay in the place between the south and north poles of the circular magnet. In step I (see Figure 2.7b), when the transistor turns on to cause the armature become north pole, the south pole of the circular magnet is pulled toward to this pole. At the same time, the north pole of the circular magnet is pushed away from this pole. Both of these two forces will keep the rotor rotating clockwise. In step II (see Figure 2.7c), when the Hall-effect sensor detects that the south pole of the magnet is coming, it will turn on the transistor to cause the armature to become the south pole and the south pole of the circular magnet is pushed away from this pole. At the same time, the north pole of the circular magnet is pulled toward to this pole. Both of these two forces will keep the rotor clockwise rotating. By switch step I and step II, the brushless motor will keep running.

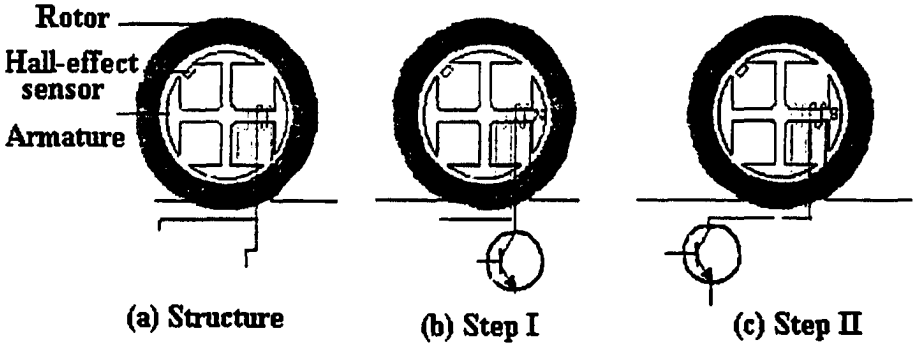


**Figure 2.7 Brushless Motor**

**Electro Magnet Valve.** Vehicle engineers have long sought an electronic method to control engine intake and exhaust valves and meet market demands for greater engine performance and improved fuel economy. On today's combustion engines, a

mechanically driven camshaft is used to operate the valves with fixed values for valve lift, timing, and duration. That is, the engine can't maintain at peak efficiency when the road or driving conditions change. The Electro Magnetic Valve system (EMV) [12][13], Figure 2.8 (FEV1999), is used to control the piston of the engine valve [11]. The EMV provides an infinite number of camshaft profiles control. That is, the EMV will allow engineers to tune and test the benefits of variable valve timing under a variety of operating conditions. The engine valves are then used to control the flow of air into a combustion engine cylinder. Normally, the EMV will consist of two electric magnets, an armature which moves between the two magnets, two springs, and an engine valve. When neither magnet is energized, the armature is held equidistant from both magnets by the two springs located on either side of the armature.

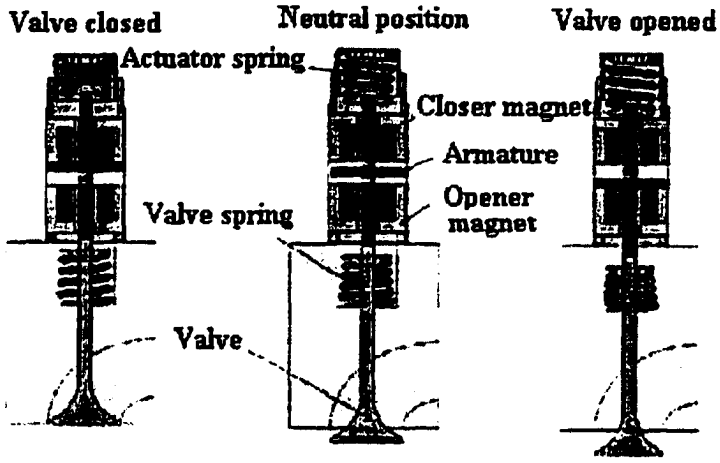


**Figure 2.8 Schematic of the EMV Systems [11]**

## 2.3 Oscillating Driver

The oscillating driver can be applied on actuators, electromagnetic valve, vibration pump, linear motor and etc. The working concept of the oscillating driver can be divided into two different types – electromagnetic force-only design [04][14][15][16] and the combination design of electromagnetic and mechanical spring forces [04][17][18][19].

The working concept for the electromagnetic force-only design was based on magnetic attractive force. The structure of this kind of design consists of two outer electrical coils and one ferromagnetic material armature (such as black iron) in the center (as seen in Figure 2.9a). The control circuit will work like an on/off switch and the device will be driven by a DC power source and the frequency could be controlled by the circuit (see Figure 2.10 for working waveforms.) The working processes will be as those seen in Figure 2.9b, c. When the stator (I) is energized (stator (II) off), it will generate an electromagnetic flux to attract the armature to move to the left side. When the stator (II) is energized (stator (I) off), it will generate an electromagnetic flux to attract the armature back to the right side. By switching between these processes, the armature will keep working back and forth. In Figure 2.13a shows an electromagnetic force design pump by PumpWorks Inc [16].

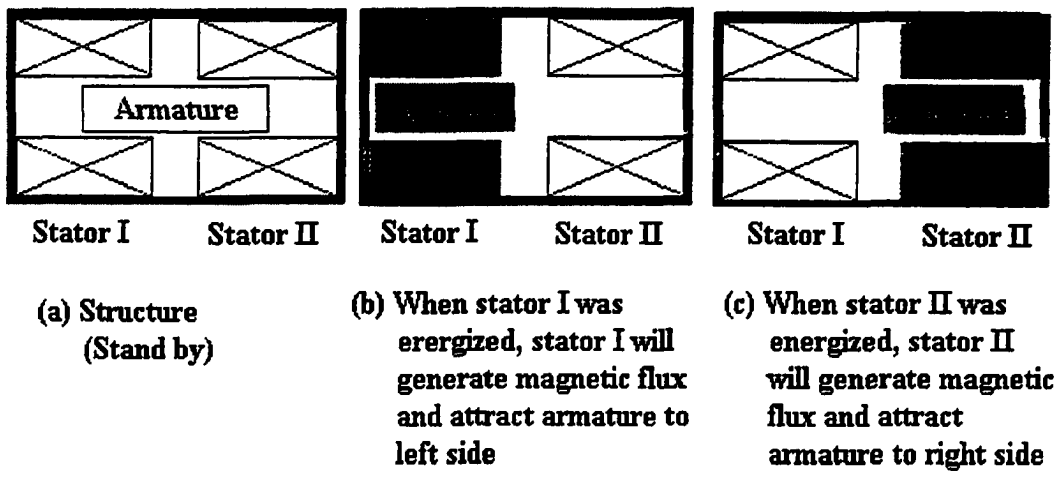


**Figure 2.9 Principle of the electromagnetic force only oscillating driver**

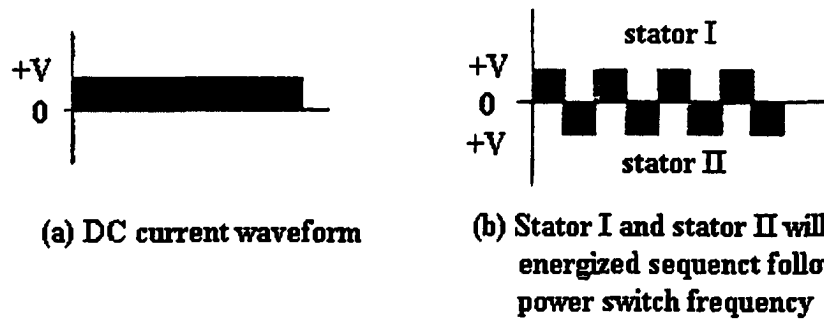


**Figure 2.10 Waveform of the electromagnetic force only oscillating driver**

For the combination design (magnet-spring), the control circuit is based on a diode. That is, the main purpose of the control circuit is to rectify the current from AC to DC. The AC current will be rectified by a single diode before connected to the coils. After the diode rectifies, only the positive half wave of current will pass through the diode to energize the coils; the electromagnetic fields generated will pull the armature and compress the spring. On the other hand, when the negative half wave of the current

is blocked by the rectify diode, the coils will lose the electromagnetic fields, and the spring will be released to push the armature back to the stand by status. See Figures 2.11, 2.12.

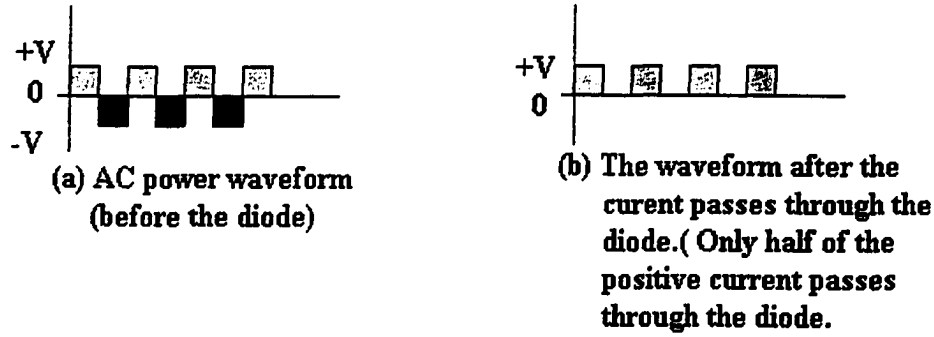


**Figure 2.11 Waveform of the magnet-spring oscillating driver**

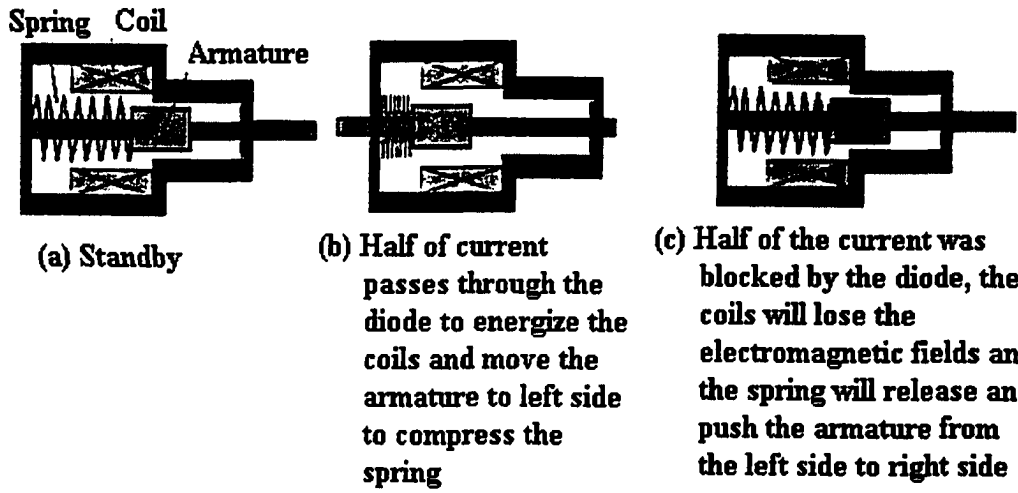


**Figure 2.12 Principle of the magnet-spring oscillating driver**

In this kind of design, the main drawbacks are complicated design and inability to change frequency (pumping speed). Since this type of design requires two forces –

mechanical spring force and electromagnetic force - the design process becomes more complicated. The designers of this type of pump often face two problems. First of all, the material choice for the spring is critical, especially for applications on small devices. The vibration generated by the spring could be too severe for some devices, too. As far as frequency is concerned, because the pump is driven by AC power source and the main purpose of the diode is to rectify the current from AC to DC, the frequency of the driver will depend totally on the frequency of the power source. That means the frequency will be set at 50 Hz or 60 Hz in USA and cannot be changed. This might limit the application of the driver (it only can have one pumping speed.) Figure 2.13b shows a commercial oscillating pump made by Depco pump company [04].

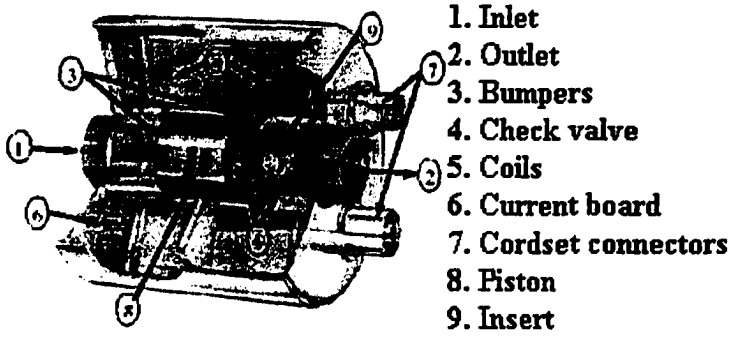


**Figure 2.13a Oscillating pump (electromagnet design) [16]**

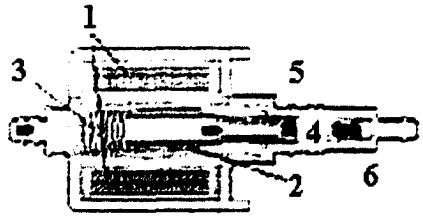


1. Solenoid coils
2. Piston
3. Piston spring
4. Inlet chamber
5. Inlet valve
6. Outlet valve

**Figure 2.13b Oscillating Pump (Electromagnet-spring design)[04]**

## 2.4 Operation Principle of Blood Pressure Monitor

Blood pressure isn't measured directly in the artery but by the arterial counter pressure squeezing the artery on which the pressure is measured.

To measure blood pressure, first, a cuff (or an arm-band) will be put on the arm and will be gradually filled with air to press the artery. A stethoscope is used to listen to the noise emitted by blood at the time of its passage in the artery below (as seen in Figure 2.14).

When the cuff is sufficiently inflated to compress the artery below, blood cannot pass any more; thus, no noise can be perceived (see Figure 2.14a), and the stethoscope becomes silent. Then, the cuff is gradually deflated and the noise now perceived defines the maximal blood pressure (see Figure 2.14b, systolic blood pressure). As the band carries on its deflation, the noise of the artery disappears again and the physician measures the pressure corresponding now to the minimal (see Figure 2.14d, diastolic blood pressure).

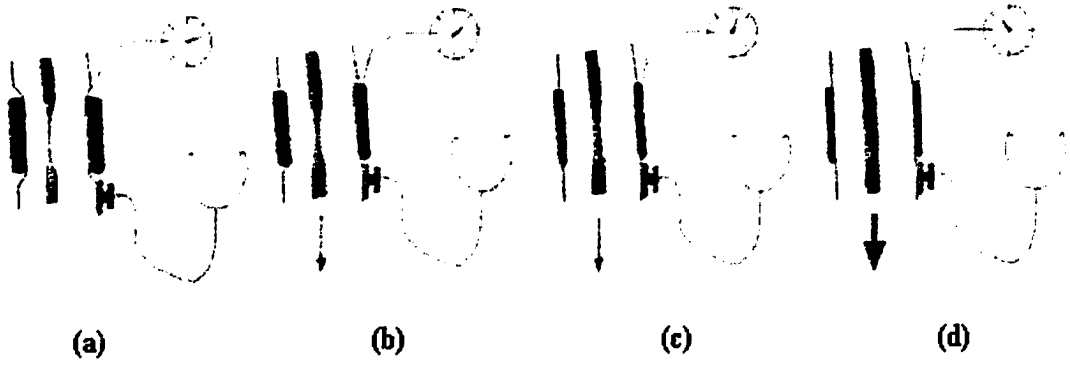


**Figure 2.14 Principle of how blood pressure monitor work [20]**

## 2.5 Current Commercial Micro Pumps

Today, there are several kinds of micro pumps available on the commercial market; however, these pumps are often too large for use in many miniaturized devices being developed. For example, the size of the AAA-Series micro air pump manufactured by Sensidyne Inc. amounts to 1.1 cubic inches [21]. It produces a free flow ranging 235 – 1410 cc/min, a pressure ranging from 0 – 6.3 psig and operates at 3, 6 or 12 VDC. The CTS-Series micro air pump made by Hargraves Technology Corporation takes up 1.2 cubic inches space [22]. It generates a free flow up to 2500 cc/min, a pressure ranging 0 – 24.0 psig and operates at 6, 9 or 12 VDC. The UNMP50 micro air pump from KNF Neuberger Inc. takes up 10.8 cubic inches space [23]. It produces a free flow up to 4000 cc/min, a pressure ranging 0 – 16.3 psig and operates at 6, 12 or 24 VDC. The 8003-0052-Series micro air pump from Thomas Pumps & Compressors Inc. requires 7.8 cubic inches storage space [24]. It offer a free flow ranging 1200 – 3000 cc/min, a pressure ranging 0 – 20.0 psig and operated at 6 or 12 VDC. The P23B-0001-00-Series micro air

pump from Oken Seiko Co. sizes 0.92 cubic inches [25]. The pump produces a free flow up to 850 cc/min, a pressure ranging 0 – 300 mmHg and operates at 3.0 VDC. These commercial pumps are either too large or too energy-demanding (requiring a high operating voltage to operate) and thus are not suitable for use in many miniaturized devices being developed today.

## 2.6 Other Related Research

The research conducted in the micro pump area is extensive. During the last decade, many kinds of micro pumps have been built based on different pumping and actuation principles. Basically, the micro pumps could divide into two major research/application fields – the Micro Electro Mechanical Systems (MEMS) based micro pumps and conventional micro pumps. For MEMS based micro pumps, research on this area was initiated in 1980 and since then numerous different pumps have been developed [26]. The MEMS based micro pumps can be manufactured from different materials, but most are made of silicon or glass. During the last decade, plastic has been shown to be a competitive alternative.

V. Gass, et. al presented a silicon micro pump with a controller [27]. Ahn and Mark developed a rotary magnetic actuator with flat integrated stator and coils operating with the rotor immersed in the fluid [28]. Maillefer and Van Lintel manufactured an implantable drug delivery system [29]. Zengerle and Ulrich presented a bidirectional silicon micro pump which consists of an electrosatically actuate diaphragm and two passive check valves [30]. Rasmussen and Zaghoul describe several operation principles

that can be integrated into biomedical analysis systems [31]. Thomas Weisenser et al presented the first rotary micro pump prototype with an outer diameter of 10 mm, and an optimized prototype with an outer diameter of only 2.5 mm was fabricated in cooperation with AGIE applying electro-discharge-machining [32]. Ansgar Wego and Lienhard Pagel present a novel micro pump based on printed circuit board technology (PCB) [33]. Cleopatra Cabuz, William R. Herb et. al presented a dual diaphragm pump which uses a conformal pumping chamber and two electrostatically actuated, structured diaphragms [34]. R Agrawal et. al designed and fabricated a silicon technology meso-scale variable capacitance motor for miniature heat pumps which integrated actuation units in the millimeter range [35]. etc.). Different pump principles are conceivable in making MEMS based micro pumps. They can generally be classified into two groups: mechanical and non-mechanical (without moving parts) [36]. At least three kinds of mechanical micro pumps have been developed: peristaltic [37], reciprocating [38-41] and rotary [41] pumps. The pumps that have attracted most attention are reciprocating diaphragm pumps, mainly because of the broad range of fluids which can be pumped and because the pumps are readily realized using silicon micro-mechanics. In non-mechanical micro pumps the electrodynamic effect, electroosmotic phenomena and ultrasonic effect are used, among others [36].

# CHAPTER 3

# DESIGN, OPERATION PRINCIPLE, PERFORMANCE CALCULATION AND SIMULATION

No matter what kind of pumping concept is applied (such as diagram, reciprocating, turbine, etc.), the driven source can be divided into two major designs on today's commercial market or researcher's area: the Rotary motor and the Oscillating driver. The Rotary motor is the most popular driving source to the pump for its simple working concept. However, the rotary motor design does have its problems; it needs extra space to store the motor, and it emits loud noise from the motor brush. Though the motor size and the noise problems have been solved by improving the strength of the permanent magnet and introducing brushless design into the motor on some applications, the major drawback about this pump is still the large size for some small application areas. The Oscillating driver is a new and highly growing research/application area in the last decade for its lack of a motor (small feature size) and easy maintenance compared to the traditional designs. Generally, the oscillating driver design will involve either electromagnetic force, or both electromagnetic force and mechanical spring force together, which is good for small applications (because the motor has been removed) and quiet (no brush and bearing was needed). The latter has the problem of its small stroke

distances (small pumping volume) and complex handling (needs to combine two different forces).

### 3.1 Design Concepts

The design of this novel micro pump can be divided into two major parts – structure/pumping concepts and driving force/control circuit. The pump structure/concept will come from the reciprocating piston pump and, the driving force and the control circuit will be a new way modified from traditional oscillating/vibrating pump.

Figure 3.1 shows the cross-sectional area of the novel micro pump. This pump consists of four main components, namely: main structure (cylinder, chamber, outlet and check valve), stators (electromagnets, coils), piston (armature - permanent magnet integrated with the inlet and check valve) and the digital control circuit (not showed in the Figure 3.1).

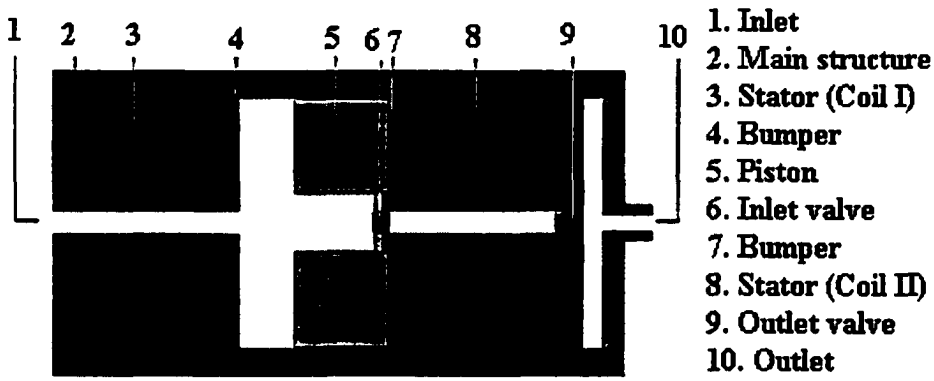


**Figure 3.1 Cross-sectional diagram of the novel micro pump**

### 3.1.1 Pump Structure and Pumping Concepts

The basic pump structure and pumping concepts of this design are similar to the reciprocating piston pump discussed in Section 2.1.2. The major difference between the traditional reciprocating piston pump and this novel design is the inlet valve. Unlike the traditional reciprocating piston pump, which has an individual inlet vale built on the main pump frame, in this novel design, the inlet valve is integrated on the piston. In this novel design, the piston includes three parts: 1) main body, 2) inlet valve frame, and 3) inlet valve (as seen in Figure 3.2). The most significant improvement of this design over its traditional counterpart is it small feature size. The inlet valve works similar to that in the traditional reciprocating piston pump. The operation of this integrated piston will be discussed in Section 3.2 later.

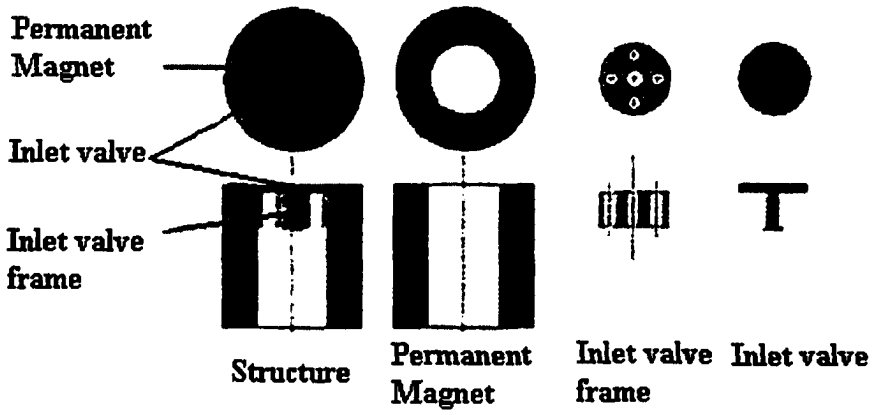


**Figure 3.2 Main components of the piston**

### 3.1.2 Driving Force and Control Circuit

The driving force and control circuit concepts of this novel design micro pump are similar to oscillating-vibrating and linear pumps widely used in industry today. However, the oscillating-vibrating and linear pumps are driven by either electromagnetic force or by the combination of electromagnetic and mechanical spring forces (as discussed in Section 2.3). The permanent magnetic force and digital control circuit (modified from traditional oscillating pump) are introduced into this design to minimize the feature size of the pump.

For the driving force, the reciprocating piston pump (see Figure 2.2 in Chapter 2) is driven by a shaft (or shafts) to transfer the energy from the power sources (such as motor, steam, water, etc). Two major problems are frequently found in this design: the feature size and efficiency.

For the feature size, the power source and the piston come from two different parts, meaning an extra space is needed to locate the driving source (such as a motor). This might not be a problem for large feature size applications, but it would appear when dealing with a small pumping system. For efficiency, since the energy for driving the piston is transferred by one or more shafts, some energy is lost during the force/direction transfer. To minimize the feature size, the motorless design is investigated in this study.

Figure 3.3 shows the main components of the traditional reciprocating piston pump and the novel design. Both motor and shaft (shafts) are removed in this novel design.

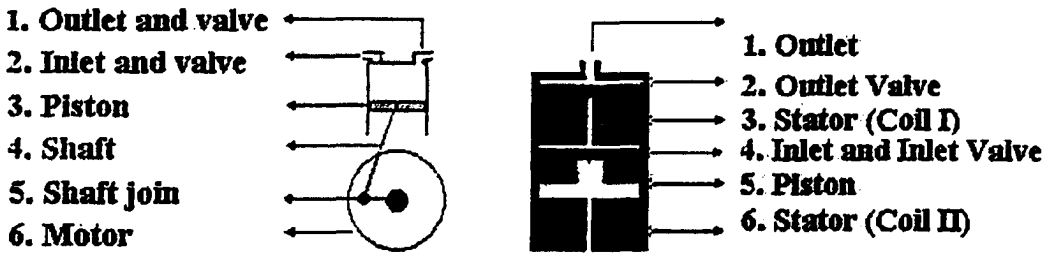


**Figure 3.3 Structures of the reciprocating pump and the novel design (not in scale)**

In this novel micro pump, the oscillating-vibrating and linear pumps' driving concepts are introduced into this design. By using the digital control circuit, the electric power is converted to electromagnetic fluxes to interact with the permanent magnetic fluxes and drive the piston directly. The motor is no longer needed and the feature size is reduced. At the same time, energy loss during the force and direction transfer is reduced as well. Figures 3.4 and 3.5 show the energy conversion processes of these two different designs. The mechanical system conversion will no longer be needed in the new design.

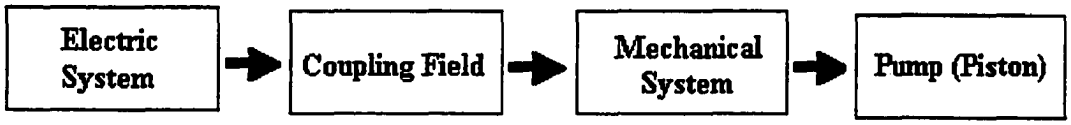


**Figure 3.4 Linked systems for traditional pump/motor design**


**Figure 3.5 Linked systems for the novel motorless design**

Using digital circuit technology to control motor and pump actions is not new. Step motors, brush/brushless motors, linear motors and others have been available for decades. For these devices, most of the digital circuit controllers use Hall-effect sensors to commutate between permanent magnet and electromagnet to translate these signals into appropriate phase currents to drive the motor or pump. The purpose of the digital control circuit in this novel micro pump is to produce an accurate train of pulses to drive the piston during forward and reverse actions to finish the pumping processes. The Hall-effect sensor is not needed in this design. Thus, the control circuit is designed to generate the sinusoidal current directly. Details about how the control circuit work will be discussed in Section 3.2.2.

## 3.2 Operation Principle

Unlike the traditional micro reciprocating piston pump driven by a rotary motor, in this novel micro pump, the pump (piston) will be directly driven by magnetic forces generated from permanent magnets and electromagnets. The working processes and the pumping speed of this pump will depend on the digital control circuit (either frequency or current strength). Changing the current direction and frequency of the two electromagnets, they generate two different forces - attractive and repulsive between the permanent magnet (armature/piston) and the electromagnets (coils/stators) (See Figure 3.6). In Figure 3.6 (b), when the stators near piston side poles are energized to become south, stator (I) will repulse piston move from left side to right side, and stator (II) will attract piston move from left side to right side. As can be seen in Figure 3.6(c), when the stators near the piston side poles are energized to become north, the stator (I) will attract

the piston from the right side to the left side, and the stator (II) will repulse the piston from the right side to the left side, as well. These two forces will move the piston in forward-reverse steps, resulting in air being pumped.

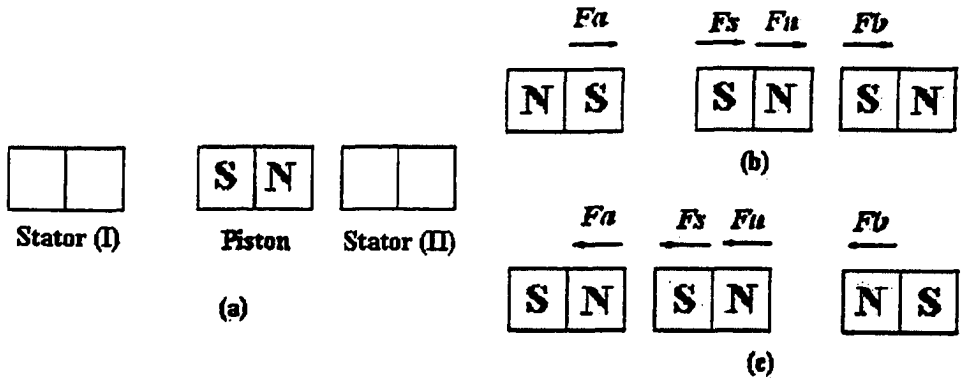


**Figure 3.6 Two possible reactions when two stators were energized by two different direction currents**

### 3.2.1 Pumping Processes

Although the pumping concepts of this novel micro pump are taken from a reciprocating piston pump, its pumping process is slightly different from that of a reciprocating piston pump due to the integration of the inlet valve onto the piston. The following sections describe how this pump works.

**Input.** As seen in Figure 3.7, when a current is applied to cause the stator (electromagnets) poles (near piston side) become south, based on the theory of the magnetism, two interaction forces will be generated between the piston and stators. Both forces will drive the piston.

1. The interactive force between the piston and the stator (II) is attractive (unlike poles), and the force between the piston and the stator (I) is repulsive (like poles). The total force working on the piston will equal to ($F_1$ + $F_2$), both pushing the piston down (because the piston is the only movable part).

2. The moving piston will generate a pressure drop between the cylinder and the outside world, a low pressure area inside the cylinder (below atmosphere) and a high pressure area outside the cylinder (equal to atmosphere). This pressure drop will cause air to flow from outside the pump into the cylinder, according to Bernoulli Theory.

3. The force generated by the air flow will force the inlet valve on the piston to be opened; at the same time, the outlet valve on the gas chamber will be closed because the gas pressure in the gas chamber will be higher than that inside the cylinder and will force the outlet valve to close.

4. The open-close actions of the valves (inlet valve opens and the outlet valve closes) and the force generated by the piston cause the air to flow into the cylinder.

Note that the force interactions between two stators are neglected because the distance between two stators is much smaller than the distances between the stators and the piston.

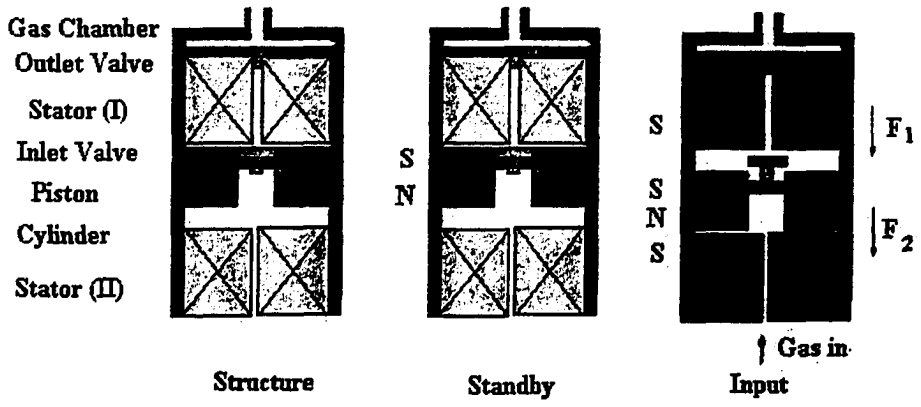


**Figure 3.7 Diagram of the input processes**

**Output.** As seen in Figure 3.8, when a current is applied to cause the stator (electromagnets) poles (near piston side) become north, based on the theory of the magnetism, two interaction forces will be generated between the piston and stators. Both forces will drive the piston.

1. The interactive force between the piston and the stator (II) is repulsive (like poles), and the force between the piston and the stator (I) is attractive (unlike poles). The total force working on the piston will equal to ($F_1$ + $F_2$), both pulling the piston up (because the piston is the only movable part).

2. The moving piston will generate some pressure drops between the cylinder, the gas chamber and the outside cylinder. Outside the cylinder will be a low pressure area (equal to atmosphere). Inside the gas chamber, the pressure will be higher than atmosphere but lower than the pressure inside the cylinder. Inside the cylinder will be a high pressure area (higher than atmosphere). These pressure drops will cause the air flow

to move from higher pressure area to lower pressure area, resulting in an air flow from cylinder to the gas chamber.

3. The valve on the piston will close (because the pressure inside cylinder is higher than the pressure outside the cylinder) and the outlet valve inside the chamber will open (because the pressure inside the cylinder is higher than the pressure inside the gas chamber).

4. The open-close actions of the valves (inlet valve closes and the outlet valve opens) and the force generated by the piston causes the air to flow out the cylinder.

Again, the force interactions between the two stators are neglected because of the distance between the two stators is much smaller than that between the stators and the piston.

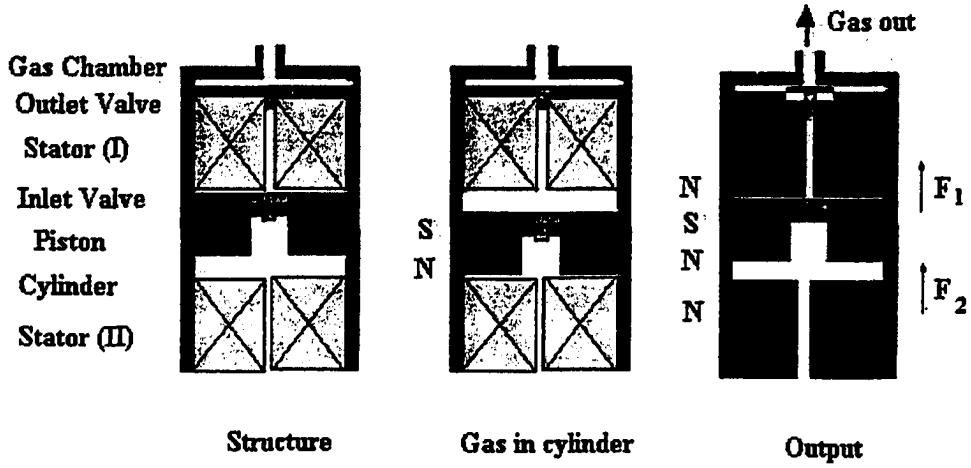


**Figure 3.8 Diagram of the output processes**

### 3.2.2 Control Circuit

Though the driving principle of this novel micro pump would appear to be like the traditional oscillating-vibrating pump or driver (as discussed in Chapter 2.3), the theory used for this novel micro pump's control circuit will be totally contrary to those used for the traditional oscillating-vibrating drivers today.

The novel micro pump was driven by a DC power source; however, based on the pumping processes discussed in section 3.2.1, a pulse current source was needed to drive the pump. The design of the control circuit in the novel micro pump is based on oscillating timer. That is, the main purpose of the control circuit is to generate an AC current (a train of pulses) from a DC current source (such as a battery). The DC current will be converted to AC current before being connected to the coils. After the DC current passes through the control circuit, two different kinds of current directions were generated during different periods of time (see Figure 3.9). During the positive half wave of a current period (see Figure 3.10b), both of the near armature sides of the coils will be energized, say south pole, the electromagnetic fields will interact with the armature: 1) the left side is attractive (unlike poles), and 2) the right side is repulsive (like poles). Both of these two forces will move the armature from the right side to the left side. On the other hand, during the negative half wave of a current period (see Figure 3.10c), both of the near armature sides of the coils will be energized, say north pole, the electromagnetic fields will interact with the armature: 1) the right side is attractive (unlike poles), and 2) the left side is repulsive (like poles). Both of these two forces will move the armature from the left side to the right side.

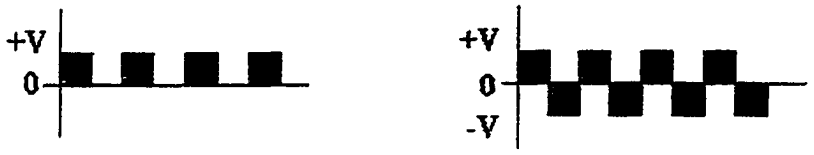


(a) The DC Power waveform (before the control circuit)

(b) The waveform after the current passes through the control circuit. (DC -> AC)

**Figure 3.9 Waveform of the novel micro pump**


(a) Stand by

(b) When the current waveform during the positive period, the armature will move to the left side

(c) When the current waveform during the negative period, the armature will move to the right side

**Figure 3.10 Oscillating principle of the novel micro pump**

There are two major advantages in this design over the traditional oscillating-vibrating driver - simplicity and high efficiency. Compared to the magnet-spring design, the mechanical spring was no longer needed; thus, the design could be much simpler (either structure or material choice). Compared to the electromagnetic force-only design, the basic structure design wasn't changed. However, because the two electromagnets would be energized at the same time, two times the electromagnetic fluxes could be generated under the same design package. That means, the feature size could be reduced

or a higher driving force could be achieved. There was another benefit for this design: pumping speed control. Since the control circuit was independent to the system, the pumping speed could be changed without changing the main structure. The only thing, one needs to do is to change some electronic parts, such as resistors or capacitors.

### 3.3 Performance Calculation

The device presented here operates on two primary concepts: the reciprocating piston pump and the interaction of magnetic fields. Based on the design requirements (see Table 3.1), the performance calculations were necessary to evaluate the possibility of this design, such as the pumping volume, current ampere, current frequency and, the magnetic forces (including permanent magnetic and electromagnetic). In the following sections, some basic performance parameters will be calculated and more detail about the magnetic fluxes calculations will be done by Excel and shown in the Appendix A. In addition, an examined with the ANSYS simulation results and experimental data appears in Chapter 6 and Appendix B.

**Table 3.1 Requirements of the pump design**

| Item | Requirements |
|---|---|
| **The pump size** | 40 mm X 10 mm X 10 mm or smaller |
| **Atmosphere** | 20 to 27°C with 30 to 80% RH |
| **Attitude** | Horizontal |
| **Rated Voltage** | 3.0 V DC |
| **Operating Voltage** | 2.2 to 3.2 V DC |
| **Operating Temperature** | 5 to 40°C with 30 to 80% RH |
| **Pressurizing Time** | Less than 10 sec to pressurize 100 $cm^3$ from 0 to 300 mmHg |
| **Max Noise** | Less than 53dB(A) at 30 cm distance while pressurization |
| **Max Pressure** | More than 350 mmHg at 3.0 V DC |

### 3.3.1 Pumping Volume and Frequency

Since the pumping concepts applied in this pump are based on the reciprocating piston pump, the following equation (Eq.2.1) used for reciprocating piston pump could be used to calculate the average pumping volume for this design.

$$Q = \eta_v * j * A * S_p * n/60 \qquad (2.1)$$

The requirement for this design is: pumping 10 $cm^3$ of gas in 10 seconds, equal to 10 $cm^3$ of gas per second. Substituting the design parameters (see Table. 3.2,) into Eq.2.1, and the pumping volume and frequency would be gotten.

**Table 3.2 Design Parameters for the pumping volume**

| Parameter | Data |
|---|---|
| Q | 10 $cm^3$/sec |
| $\eta_v$ | 0.90 for small pump |
| J | 1 (piston) |
| A (piston radius is 3 mm) | 28.27 $mm^2$ |

For example, assume the stroke distance is 6 mm. Substituting this and data from Table 3.2 into Eq.2.1,

$$10\ cm^3/sec * (10^3\ mm^3/cm^3) = 0.9 * 1 * 28.27\ (mm^2) * 6\ (mm) * n/60$$

The n value (rpm) was gotten at 3929. Using the same method, the stroke values needed for different rpm could be gotten, too. The results are seen in Table 3.3.

**Table 3.3 Calculation results of the pumping frequency**

| Stroke Distance (mm) | | Frequency | | Stroke Distance (mm) | | Frequency | |
|---|---|---|---|---|---|---|---|
| | | Rpm | Hz | | | rpm | Hz |
| Sp | 1.0 | 23574 | 396 | Sp | 3.0 | 7859 | 131 |
| | 1.5 | 15716 | 264 | | 4.0 | 5894 | 98 |
| | 2.0 | 11787 | 198 | | 5.0 | 4715 | 79 |
| | 2.5 | 9430 | 158 | | 6.0 | 3929 | 66 |

### 3.3.2 Driving Force

After the stroke distances and the frequencies were defined, the next step was to calculate the total force needed to achieve these designs. Newton's Laws of Motion and the liquid pressure principle were applied to calculate the minimum force needed to drive the piston.

Newton's Laws of Motion, Eq.3.1, 3.2

$$S = 1/2 * a * t^2 \quad (3.1)$$

$$F = m * a \quad (3.2)$$

Here

**S:** working distance (stroke distance)

**a:** acceleration

**t:** time

**F:** force

**m:** mass

The total mass for the piston would be the permanent magnet plus the valve. The dimension for the piston was (6.0 mm * 3.0 mm * 6.0 mm) and the density of the permanent magnet (sintered NdFeB permanent magnet) was 7.5 g/cm$^3$. Since there would have some friction between the piston and the cylinder wall, the friction coefficient 0.2 was assumed. Based on the assumptions above, the final mass the force needs to drive would be 1.35 g. Using the mass, stroke distances and the frequencies into above equations, the total forces needed to drive the piston under vacuum condition could

be calculated. For example, $S_p$ = 6mm; f = 66Hz; t = 0.015 sec, t' = 0.0075 sec (because 0.0015 was for run travel, really the time for one stroke distance was just half of it).

$$S = \frac{1}{2} a*t^2 \Rightarrow 0.6 = \frac{1}{2} *a * 0.0075^2$$

$$a = 21333 \text{ (cm/sec}^2\text{)}$$

$$F = m*a = 1.35 * 21333 = 28800 \text{ (dyne)}$$

Using the same calculations, the remaining results would be calculated, as seen in Table 3.4

**Table 3.4 Forces needed under different setups**

| Stroke Distance $S_p$ (mm) | Frequency (Hz) | Time (Sec) | Acceleration (cm/sec$^2$) | Force (Dyne) |
|---|---|---|---|---|
| **6.0** | **66** | 0.0075 | 21333 | 28800 |
| **5.0** | **79** | 0.006 | 27777 | 37500 |
| **4.0** | **98** | 0.005 | 32000 | 43200 |
| **3.0** | **131** | 0.0038 | 41551 | 56093 |
| **2.5** | **158** | 0.003165 | 49914 | 67384 |
| **2.0** | **198** | 0.002525 | 62739 | 84698 |
| **1.5** | **264** | 0.001894 | 83630 | 112900 |
| **1.0** | **396** | 0.001263 | 125379 | 169261 |

From the steady liquid pressure principle (Eq.3.3, 3.4), the total force needed under the pumping processes (the highest pressure condition) could be calculated,

$$\mathbf{P = F/A} \tag{3.3}$$

$$\mathbf{F = P * A} \tag{3.4}$$

Here

**P**: Pressure

**F**: Force

**A**: Area

The final requirement for the pressurization was 350 mmHg. Based on the liquid pressure principle, the pressure was formed by force per square area and the cross-section area of the piston in this design was 28.27 $mm^2$. Substituting them into the Eq.3.3 and 3.4, the force needed to achieve this pressure is given by:

$$P = 350 \text{ mmHg} = 0.4605 \text{ atm} = 446650 \text{ nt/m}^2 = 4665 \text{ dyne/mm}^2$$

$$F = 4665 * 28.27 = 131880 \text{ (dyne)}$$

Adding this number into Table 3.4 gives the total force needed to achieve this design. (See Table 3.5)

**Table 3.5 Total force needed under different setups**

| Stroke Distance $S_p$ (mm) | Frequency (Hz) | Force (Dyne) | Stroke Distance $S_p$ (mm) | Frequency (Hz) | Force (Dyne) |
|---|---|---|---|---|---|
| **6.0** | **66** | 160680 | **2.5** | **158** | 199264 |
| **5.0** | **79** | 169380 | **2.0** | **198** | 216578 |
| **4.0** | **98** | 175080 | **1.5** | **264** | 244780 |
| **3.0** | **131** | 187973 | **1.0** | **396** | 301141 |

### 3.3.3 Magnetic Flux and Force

Based on the design concepts, this novel pump would be driven directly by the magnetic force and the force needed to drive the piston from Section 3.3.2. The next step is to design a magnetic circuit that would generate enough force to match the design requirements. The basic setup for this design (see Figure 3.11 and Table 3.6) would include one piston (permanent magnet) and two stators (electromagnets). Two kinds of magnetic forces would be involved in this design – permanent magnetic force and electromagnetic force. Based on this setup and magnetism, there will be three different force interactions between the piston and the stators during the operation – $F_1$: stator (I) V.S piston; $F_2$: stator (II) V.S piston and $F_3$: stator (I) V.S stator (II). Since the strength of $F_3$ was much smaller than $F_1$ and $F_2$ (because the magnetic flux interaction between two magnets was proportional to $1/(\text{distance})^2$ and, the distance between Stator (I) and

stator (II) was much larger than stator (I) V.S piston and stator (II) V.S piston), it would be neglected in this design. And more, if the reluctance inside the cores was neglected (either ferrous or nonferrous cores), and the rare earth magnet (piston) with straight demagnetization line was applied, then the magnetic circuit of the piston (permanent magnet) and stators (electromagnets) were in a linear system. In other words, the fields excited by the piston magnet and two stator coil currents could be calculated individually and then be summed together directly. In this design, the magnetic circuit will be assumed in linear system.

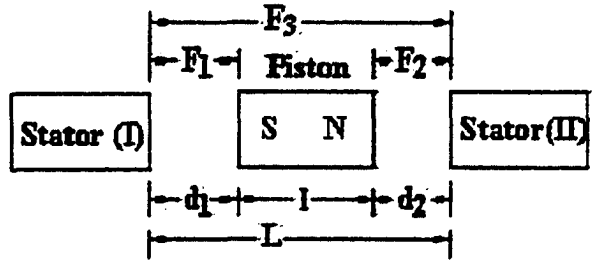


**Figure 3.11 Geometric modeling setup and force relationship**

**Table 3.6 Description of Figure 3.11**

| | Description |
|---|---|
| $F_1$ | The interaction force between Stator (I) and Piston. |
| $F_2$ | The interaction force between Stator (II) and Piston |
| $F_3$ | The interaction force between Stator (I) and Stator (II) |
| L | The distance between two Stators ($L = d_1 + d_2 + l$) |
| l | The length of the Piston (permanent magnet.) |
| $d_1$ | The distance between Stator (I) and the Piston |
| $d_2$ | The distance between Stator (II) and the Piston |

**Permanent magnetic force.** Permanent magnetic force would be the major force source in this design. The magnetic flux generated by the permanent magnet would interact with the electromagnetic fluxes generated by stators to drive the piston. According to Biot-Savart's law, the magnetic flux density along the axis of the permanent magnet could be calculated with the dimension and residual induction ($B_r$) of the material. Two kinds of different geometric models have been reviewed (see Figure 3.12). For an external view, the Cylinder Tube Magnet Magnetized Axially (Figure 3.12a) is much like the design presented in this study; however, because the actual magnetic fluxes interaction area in the design are not at the center point of the magnet but at the place surrounding the center area, the Cylindrical Magnet Magnetized Axially (Figure 3.12b) and Eq.3.5 was the model applied in the following calculations.

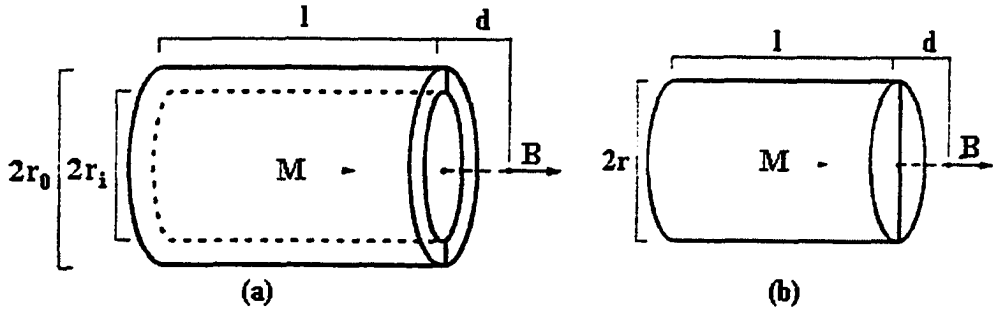


**Figure 3.12 Two different permanent magnet geometric models** [42]

$$B = \frac{B_r}{2}\left[\frac{d+l}{\sqrt{(d+l)^2+r^2}} - \frac{d}{\sqrt{d^2+r^2}}\right] \tag{3.5}$$

Here

$B_r$: Flux density (Gauss) of the permanent magnet

**r:** The radius (in inch)

**l:** The length of the permanent magnet (in inch)

**d:** Distance from the permanent magnet pole surface to target place (in inch)

In Figure 3.11, when a current was applied to energize the Stator (I) to cause its right end side pole phase to become north, the flux density at the center point of Stator (I) right end side surface generated by Piston's south pole (Eq.3.6), $B_S$

$$B_S = \frac{B_r}{2}\left[\frac{d_1+l}{\sqrt{(d_1+l)^2+r^2}} - \frac{d_1}{\sqrt{d_1^2+r^2}}\right] \tag{3.6}$$

Here,

**$B_r$:** 12130 Gauss

**l:** 0.236 inch

**r:** 0.118 inch

**$d_1$:** 0 inch (for the pole surface to get the maximum flux density from this side.)

Applying the data above into Eq.3.6, the $B_S$ could be gotten at 5424.701 Gauss. The magnetic flux generated by the piston's left end side (south pole) would attract the stator (I) and the direction was from right side to left side (because stator (I) was stuck on the main structure and the piston was the only movable part, that means the piston would move from right side to left side). In the same fashion, when a current was applied to energize the stator (II) to cause its left end side pole phase to become north, the flux density at the center point of the stator (II) left end side surface generated by the piston's north pole (Eq.3.7), $B_N$

$$B_N = \frac{B_r}{2}\left[\frac{d_2+l}{\sqrt{(d_2+l)^2+r^2}} - \frac{d_2}{\sqrt{d_2^2+r^2}}\right] \tag{3.7}$$

Here,

**$d_2$:** 0.236 inch (the farthest point between piston and stator (II))

Solving Eq.3.7, the $B_N$ could be gotten at 459.213 Gauss. The magnetic flux generated by the piston's right end side (north pole) would repulse the stator (II) from the right side to the left side (because the stator (II) was stuck on the main structure and the piston was the only movable part, meaning, the piston would move from the right side to the left side).

After two sides individual flux density were gotten, they were added together to get the total flux density working on the piston by the permanent magnet in the magnetic circuit, 5883.914 Gauss. The total force working on the system could be gotten by using Eq.2.9

$$F = \frac{B_r^2 \times A}{8\pi} \tag{2.9}$$

$$F = 5883.914^2 * \pi(0.3^2 - 0.15^2)/8\pi$$

$$F = 292110 \text{ (dyne)}$$

**Stators – Electromagnetic Flux and Field.** Someone might wonder, based on the calculation results in Section 3.3.2 and 3.3.3.1, if the force generated by the permanent magnet was already large enough to drive the piston, why were the other two stators needed? There were two reasons that two stators were needed for this design. First, the magnetic flux couldn't work on nonmagnetic material and it couldn't work alone. The magnetic force needed to work like a dipole, and if there wasn't any other magnetic source or magnetic material, nothing would happen no matter how strong the

magnetic source was. Secondly, based on the results in Section 3.3.2 and 3.3.3.1, it's clear that just using one stator would create enough force to push the piston from one side to another side. However, there wouldn't be enough force to attract it back and it would be stuck at one side.

The purpose of the two stators was to create another magnetic source so that could interact with the permanent magnet to generate enough force to drive the piston. The design of the stators was two individual solenoid electromagnets (see Figure 3.13.) Based on the electromagnetism discussed in Chapter 2.2, for easy calculation, the magnetic flux density (B) inside a solenoid in vacuum (Eq.2.6) could be expressed as (Eq.3.8). And the number of the turns for a given length core and wire grade could be expressed as Eq.3.9.

$$B = \mu_0 \times \mu_r \frac{NI}{l} \tag{3.8}$$

$$N = \frac{R_o - R_i}{D_{wire}} \times \frac{1}{D_{wire}} \tag{3.9}$$

Here

**B:** Electromagnetic Flux Density (Tesla)

$\mu_o$: Permeability ($4\pi * 10^{-7}$ weber/ampere-meter)

$\mu_r$: Relative Permeability (dimensionless, depend on the core material)

**N:** Number of the turns

**I:** Current (Ampere)

**l:** Length of solenoid (Meter)

$\mathbf{R_i}$: Solenoid inside radius

$\mathbf{R_o}$: Solenoid outside radius

$\mathbf{D_{wire}}$: Diameter of the wire

To generate enough electromagnetic flux to interact with the permanent magnet, the following data will be used for the prototype testing. For optimizing the data, more details would be presented in Chapter 6.

Assume,

$\mu_r$: For air core: 1

**I:** 800 mA

**l:** 13.00 mm (0.013 m)

$\mathbf{R_i}$: 0.30 mm

$\mathbf{R_o}$: 3.00 mm

$\mathbf{D_{wire}}$: 0.388 mm (Using AWG 27 wire, maximum support current up to 968 mA)

Based on the wire diameter, solenoid length and diameter, the number of turns (N) could be calculated by Eq.3.9,

$$N = (2.7/0.388) * (13.00/0.388) = 233 \text{ (turns)}$$

Apply the assumption data and number of coil turns from Eq.3.9 above into Eq.3.8.

$$B = 4\pi * 10^{-7} * 1 * 233 * 0.80/0.013$$

$$B = 0.0180182 \text{ (Tesla)} = 180.182 \text{(Gauss)}$$

Apply the flux density B (180.182 Gauss) (setup as seen in Figure 3.11) into Eq.3.6, 3.7, and 2.9 to get the forces working on the piston by two stators. From Eq.3.6, when a current was applied to energize the Stator (I), the flux density at the center point of the piston's left end side surface generated by the Stator (I) was (Eq.3.10), $B_a'$

$$B_a' = \frac{B_E}{2}\left[\frac{d_1+l}{\sqrt{(d_1+l)^2+r^2}} - \frac{d_1}{\sqrt{d_1^2+r^2}}\right] \tag{3.10}$$

Here,

$\mathbf{B_E}$: Electromagnetic Flux Density, 180.182 Gauss

**l:** Length of the electromagnet, 0.511 inch

**r:** 0.118 inch

$\mathbf{d_1}$: 0 inch (for the pole surface to get the maximum flux density from this side.)

$B_a'$ was gotten at 87.781 Gauss. The stator (I) would attract the piston from the right side to the left. From Eq.3.7, when a current was applied to energize the stator (II),

the flux density at the center point of the piston right end side surface generated by Stator (II) was (Eq.3.11), $B_b'$

$$B_b' = \frac{B_E}{2}\left[\frac{d_2+l}{\sqrt{(d_2+l)^2+r^2}} - \frac{d_2}{\sqrt{d_2^2+r^2}}\right] \tag{3.11}$$

Here,

$d_2$: 0.236 inch (the farthest point between the piston and stator (II))

The $B_b'$ was 8.408 Gauss. The stator (II) would repulse the Piston from the right side to the left.

After two sides of the individual electromagnetic flux density was calculated, they were added together to get the total flux density working on the piston by the electromagnets in the magnetic circuit, 96.189 Gauss. At the same time, the total force working on the system could be calculated using Eq.2. 9

$$F = 96.189^2 * \pi(0.3^2 - 0.03^2)/8\pi$$

$$F = 103.048 \text{ (dyne)}$$

**Total Force Generated By Magnetic Flux.** Based on the calculations in Section 3.3.3.1 (permanent magnetic force, 292110 dyne) and Section 3.3.3.2 (electromagnetic force, 103.048 dyne), the total force generated by magnetic fluxes was 292213.048 dyne. This number was much higher than the force desired to drive the piston (from Section 3.3.2) and it provided the confidence to make a prototype and continue further testing.

## 3.4 Numerical Simulation of Magnetic Flux/Field

Numerical simulation is a widely used technique on today's engineering research area. The best benefit of simulation is that it can predict problems that might occur during the prototyping and further evaluation. In this section, the simulation model, the results of this design, and the comparisons between the calculation results in Section 3.3.3 will be presented.

### 3.4.1 Finite Element Method

The finite element method is commonly used for analyzing structures and continua. It was originally developed as a method for stress analysis, but today it is also used to solve problems in electric and magnetic fields, fluid flow, heat transfer, lubrication and many other fields [43]. The finite element method models a structure as an assemblage of small parts (elements). Each element has a simple geometry and therefore is easier to analyze than the actual structure. A complicated solution is approximated by a model that consists of piecewise continuous simple solutions. The elements are called "finite" to distinguish them from differential elements used in calculus. The type of element used in the model and the number of elements are important for the accuracy of the solution.

The finite element method is very versatile. It can be applied to various physical problems where the analyzed body can have arbitrary shape, loads and support conditions. Another attractive feature is the close physical resemblance between the

actual structure and its finite element model. A disadvantage of the finite element method is that a specific numerical solution is found for a specific problem. No closed form solution permits an analytical study of the effects of changing the different parameters. It is also necessary to have experience and good engineering judgment in order to define a good model.

### 3.4.2 Magnetic Flux/Field Simulations by ANSYS Software

ANSYS/Multiphysics combines the power of matrix- and load-vector coupling to represent the "physical fields" required for accurate, reliable simulation results in applications ranging from cooling systems and power generation, to biotechnology and MEMS. The software easily simulates complex thermal/mechanical, fluid/structural and electrostatic/structural interactions, and includes the complete range of powerful ANSYS iterative, direct and engineering solvers [44].

The ANSYS/Multiphysics program uses Maxwell's equations as the basis for magnetic field analysis. The primary unknowns (degrees of freedom) that the finite element solution calculates are either magnetic potentials or flux. Other magnetic field quantities are derived from these degrees of freedom. Depending on the element type and element option chosen, the degrees of freedom may be scalar magnetic potentials, vector magnetic potentials, or edge flux. [45]

The following types of functions will be used in this study:

- 2-D static magnetic analysis, analyzing magnetic fields caused by direct current (DC) and permanent magnets. Using the vector potential formulation.
- 3-D static magnetic analysis, analyzing magnetic fields caused by direct current (DC) and permanent magnets. Using a scalar potential approach.

For more detail about the analysis types, see the ANSYS/Multiphysis operation guide for Electromagnetic Field Analysis.

### 3.4.3 Approach and System Modeling

For using a signal iteration linear analysis, the magnetic flux produced by the coil current will be assumed to be as small as possible. That is, no saturation will happen in the cores (either air or iron cores). And, to keep the simulation simple, the flux leakage out of the perimeter of the model will be assumed to be negligible, too (the overall simulation parameters see Table 3.10).

The air gap is modeled so that a quadralateral mesh is possible. A quadralateral mesh allows for a uniform thickness of the air elements adjacent to the piston where the virtual work force calculation is performed [45]. The current will be input in the form of current density (current over the area of coil). Based on the assumption that there is no leakage at the perimeter of the model, the flux will be acting parallel to this surface. This assumption is enforced by the "flux parallel" boundary condition placed around the model.

The driving force of the novel Micro Pump comes from two stators (electromagnets) and one armature/piston (permanent magnet). The permanent magnet

will work as an armature moving between these two stators. The basic setup as shows in Figure 3.13.

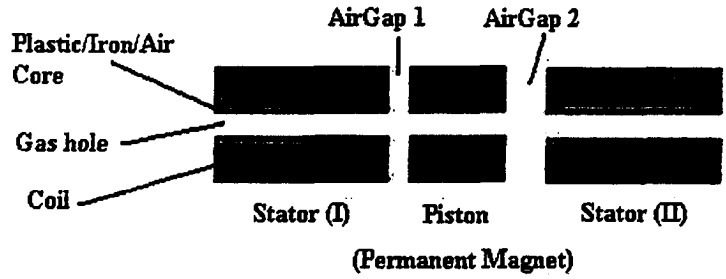


**Figure 3.13 Setup sketch of the three magnetic sources**

Based on the design principle and materials choices (for coil cores), the simulation model in this project will include three identified parts: permanent magnetic flux/field (for the piston), electromagnetic flux/field in a ferrous solenoid and electromagnetic flux/field in a nonferrous solenoid (for the electromagnetic magnet). To simplify the problem, each simulation will be done individually first and put together for the final model after that.

### 3.4.3.1 Permanent Magnetic Flux/Field

**Overview**

Analysis Type: Magnetic Field Analysis (ANTYPE=0)

Element Type: Tetrahedral Coupled-Field Solid Elements (SOLID98)

Method: Scalar Potential Approach

**Description**

Assuming an ideal circuit with no flux leakage. A permanent magnet circuit consists of a highly magnetic flux density permanent magnet (as see in Figure 3.14). In this micro pump, the permanent magnet will be the major magnetic flux source to drive the pump. To get the maximum magnetic flux density (at the surface of the permanent magnet, $S_p$ = 0 mm) and minimum magnetic flux density (at the maximum stroke distance point, $S_p$ = 6 mm), the simulation will determine the magnetic flux density at the center of the magnet end surface and at a point 6 mm from the end of the magnet.

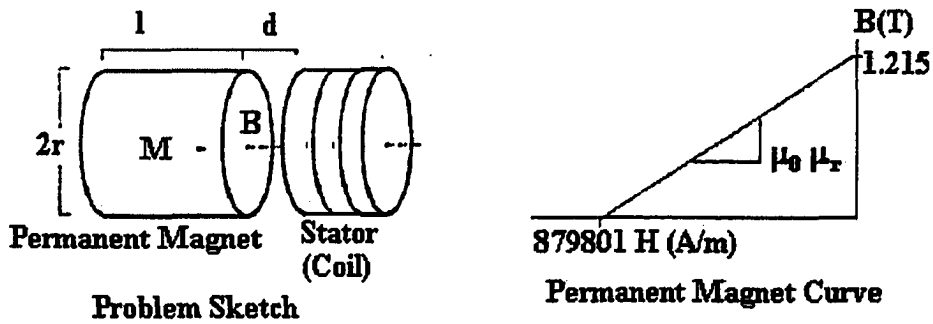


**Figure 3.14 Problem setup sketch for permanent magnet (Piston)**

**Table 3.7 Material and geometric properties for permanent magnet simulation**

| Material properties | Geometric properties |
|---|---|
| $B_r$ = 1.213 Tesla | l = 6.00 mm |
| $H_c$ = 879801 A/m | r= 3.00 mm |
| Θ = 0°, along X axis | d = 6 mm (Max stroke distance) |
| $\mu_r$ | 1 (air) |

**Analysis Assumptions and Modeling Notes**

The problem is solved using coupled-field solid elements (SOLID98). The permanent magnet is polarized along a line at Θ = 0° to the X-axis. The coercive force components are calculated as $H_c$ =879801 (A/m, from company data). The permanent magnet relative permeability, $\mu_r$, is calculated as

$$\mu_r = \frac{B_r}{\mu_0 \times H_c} = \frac{1.213}{\left(4 \cdot \pi \times 10^{-7}\right)(879801)} = 1.0971$$

The permeability of air is assigned a value $\mu_r$ = 1

Since the device is symmetric, only half of the circuit is required for modeling. At the symmetry plane the flux lines are orthogonal, so a flux-normal (Φ = 0) boundary condition is applied. With no leakage in the system, all the flux flows along a path circumventing the circuit. For setup and results, see Figure 3.15 and 3.16.

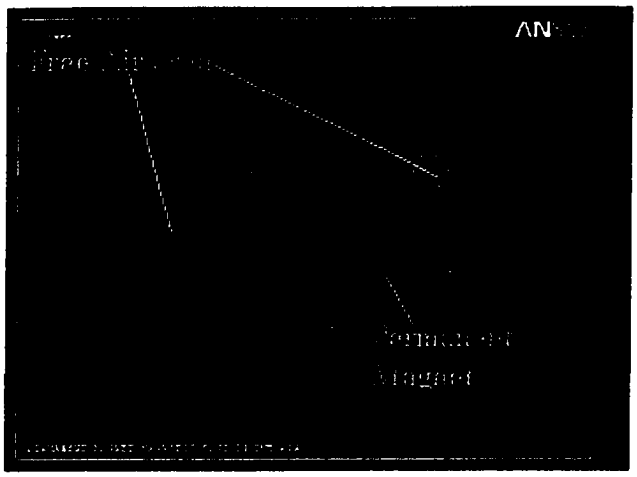

**Figure 3.15 Setup for permanent magnet simulation**

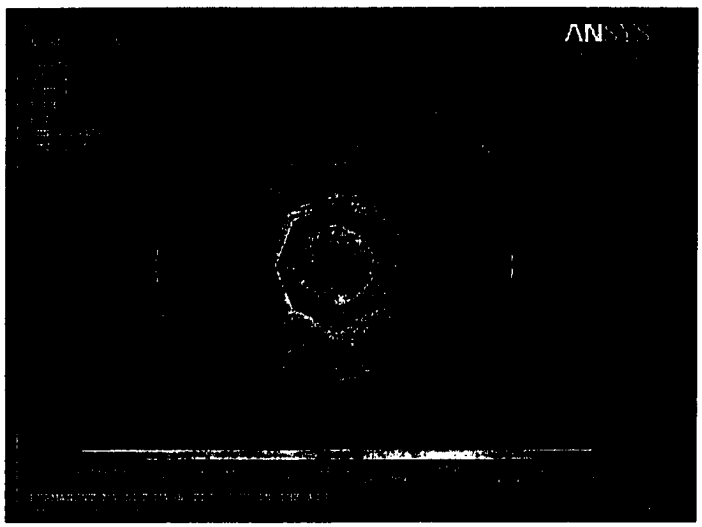

**Figure 3.16 Result for permanent magnet simulation**

**Results Comparison**

| Using SOLID98 | Target | ANSYS | Ratio |
|---|---|---|---|
| B (Tesla, Max) | 1.213 | 1.15 | 0.95 |
| B (Tesla, Min) | - | 2.94E-6 | |

### 3.4.3.2 Electromagnetic Flux/Field

To simply the simulation and use less time to solve the problem, the simulation used for electromagnet (stator) will be a 2-D axisymmetric model.

**Electromagnetic Flux /Field by**
**Ferromagnetic Core**
**in Solenoid**

**Overview**

Analysis Type(s): Static Magnetic Field Analysis (ANTYPE=0)

Element Type(s): Higher-Order Element (PLANE53)

Method: Vector Potential Formulation

**Description**

A ferromagnetic solenoid is wound with N turns of AWG. 27 enameled wire and carries a current I (setup as seen Figure 3.17, 18). Similarly, since the needed data for this design is to get the maximum and minimum electromagnetic fluxes that acted on the piston (permanent magnet), the simulation will determine the magnetic flux density at the center of the coil end surface and at a point 6 mm from the end of the coil.

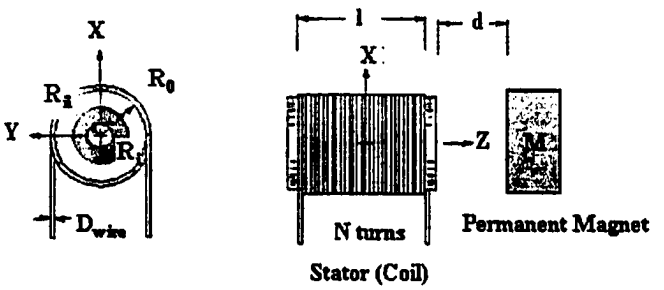


**Figure 3.17 Ferromagnetic core solenoid problem sketch**

**Table 3.8. Material and geometric properties of for ferromagnetic core simulation**

| Material properties | Geometric properties |
|---|---|
| $\mu_r = 2500$ (core)<br>$\mu_r = 1$ (air) | l = 13.00 mm |
| I = 800 mA | $R_0 = 3.00$ mm<br>$R_i = 1$ mm<br>$R_{ii} = 0.5$ mm |
| $\Theta = 0°$, along Z-axis | D = 6 mm |
| N = 233 (turns) | |

**Analysis Assumptions and Modeling Notes**

Since the core material has finite permeability, air is modeled to a small distance away from the core. The open boundary is modeled with an infinite surface element at the edge of the air region. The model employs 1/2 symmetry (about the X and Y planes). The current to be input was formed as current density (current over the area of the coil). The result as seen in Figure 3.19)

**Results Comparison**

| | Target | ANSYS | Ratio |
|---|---|---|---|
| **B (Tesla, Max)** | 2.435 | 2.436 | 1.0 |
| **B (Tesla, Min)** | - | 1.43E-5 | - |

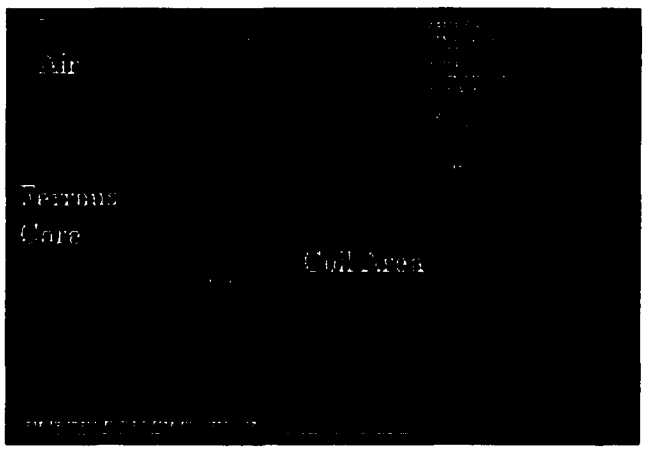


**Figure 3.18 Ferromagnetic Core Simulation Setup**

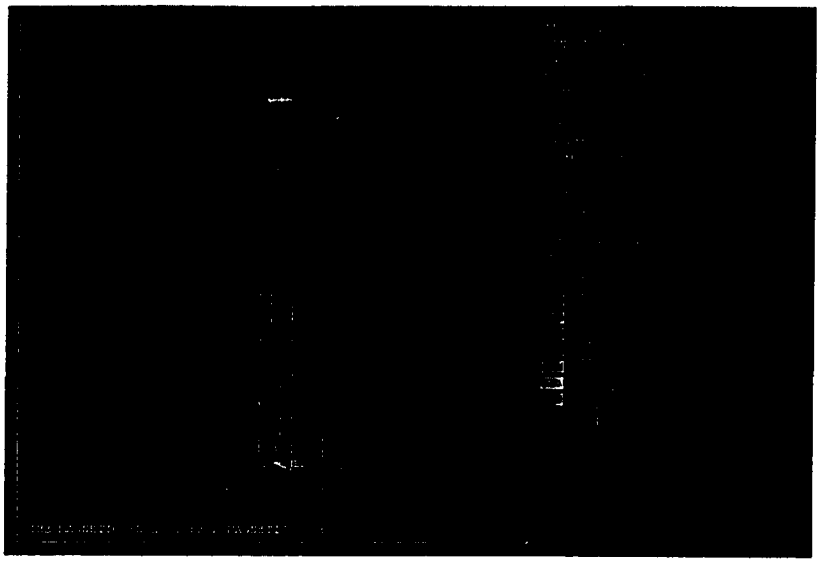

**Figure 3.19 Simulation result for ferromagnetic core**

**Electromagnetic Flux/Field in a Nonferrous Solenoid**

**Overview**

Analysis Type(s): Static Magnetic Field Analysis (ANTYPE=0)

Element Type(s): Higher-Order Element (PLANE53)

Method: Vector Potential Formulation

**Description**

A nonferrous solenoid (air core) is wound with N turns of AWG. 27 enameled wire and carries a current I. (see Figure 3.20, 3.21). The magnetic flux density is determined on the centerline at the center of the coil the end of the coil at a point 6 mm from the end of the coil.

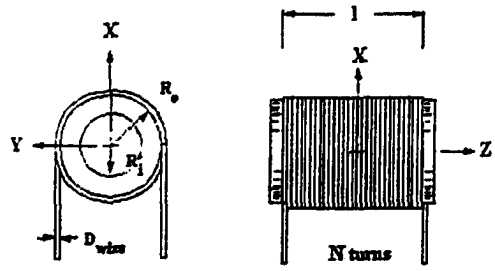


**Figure 3.20 Problem setup sketch for nonferrous solenoid[45]**

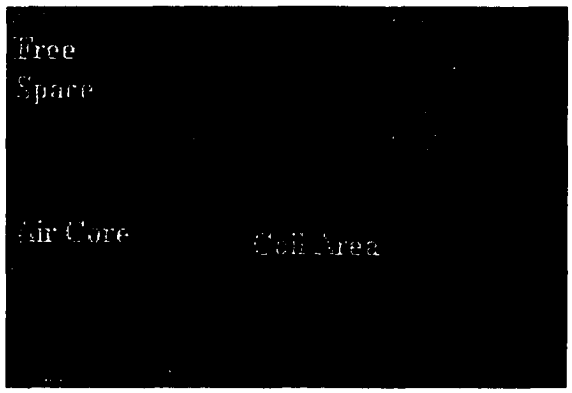


**Figure 3.21 Setup for nonferrous core simulation**

**Table 3.9 Material properties and geometric properties for nonferrous core simulation**

| **Material properties** | Geometric properties |
|---|---|
| $\mu_r = 1$ (air) | l = 13.0 mm |
| I = 800 mA | $r_0$= 3.00 mm<br>$r_i$ = 0.3 mm |
| $\Theta = 0°$, along Z-axis | d = 6 mm |
| N = 233 (turns) | |

**Analysis Assumption and Modeling Notes**

The number of turns is N = (2.7/0.388) * (13.00/0.388) = 233 (turns). Therefore, N x I = 186.4 Ampere-turns. Since no ferromagnetic materials are presented, the field is due to induced magnetization, $H_m = 0$, and thus no scalar potential is required. The total field can be determined from the numerical integration of the coil source field upon specification of the coil with the current source element (Plane53). Since the field is symmetric, only half of the area is needed or the simulation. The result is seen in Figure 3.22.

**Results Comparison**

| | **Target** | **ANSYS** | **Ratio** |
|---|---|---|---|
| **$B_Z$ (Gauss, Max)** | 180.182 | 180.18 | 1.0 |
| **$B_Z$ (Gauss, at d = 6.00 mm)** | 8.408 | - | |

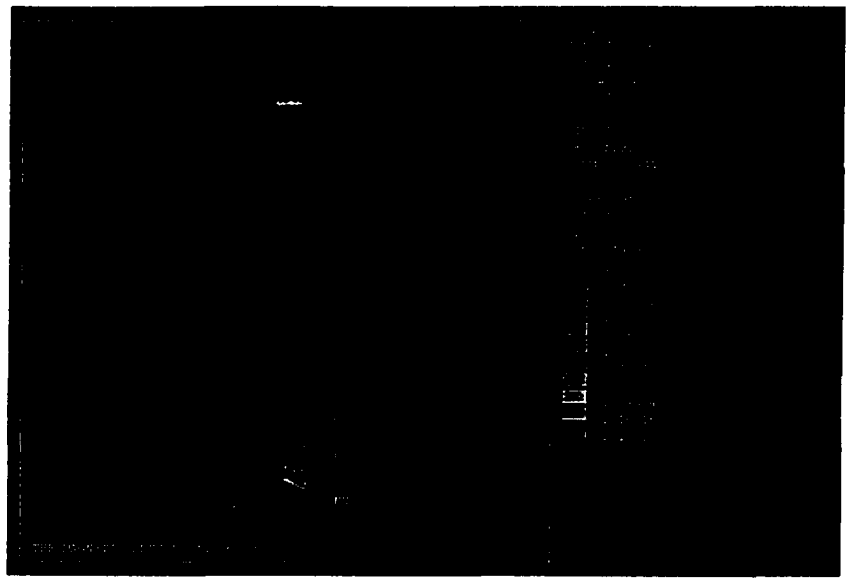

**Figure 3.22 Simulation result of nonferrous core**

### 3.4.3.3 Combination Design

**Overview**

Analysis Type(s): Static Magnetic Field Analysis (ANTYPE=0)

Element Type(s): Higher-Order Element (PLANE53)

Method: Vector Potential Formulation

**Description**

A half ferromagnetic and half nonferrous solenoid is wound with N turns of AWG. 27 enameled wire and carries a current I (setup as see Figure 3.23, 3.24). The magnetic flux density is determined on the centerline at the center of the coil the end of the coil at a point 6 mm from the end of the coil. The result is seen in Figure 3.25.

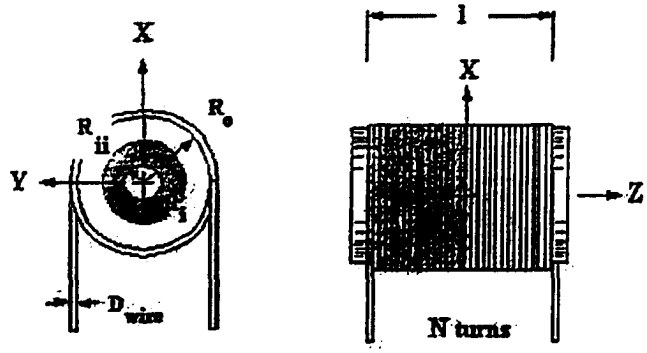


**Figure 3.23 Sketch of half ferromagnetic and half nonferrous core**

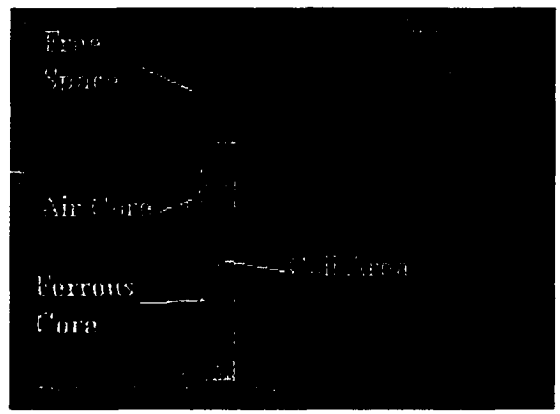


**Figure 3.24 Setup for half ferromagnetic and half nonferrous core simulation**

**Results Comparison**

| | Target | ANSYS | Ratio |
|---|---|---|---|
| **B (Gauss, at d = 0.0 mm)** | 947.156 | 948.24 | 1 |
| **B (Gauss, at d = 6.0 mm)** | -- | -- | -- |

**Figure 3.25 Result of the half ferromagnetic and half nonferrous core simulation**

**Table 3.10 Simulation Parameters**

| Symbol | Value | Description |
|---|---|---|
| $\mu_0$ | $4\pi*10^{-7}$ (H/m) | Permeability of free space |
| $R_{pi}$ | 1.00 mm | Permanent magnet inside radius |
| $R_{po}$ | 3.00 mm | Permanent magnet outside radius |
| $R_{ci}$ | 1.00 mm | Coil inside radius |
| $R_{co}$ | 3.00 mm | Coil outside radius |
| $R_{ii}$ | 0.3 mm | Ferromagnetic core inside radius |
| $R_{io}$ | 1.00 mm | Ferromagnetic core outside radius<br>(Air core radius) |
| $G_1$ | Between 0.0 to 6 mm | Air gap 1 (between Stator (I) and Piston) |
| $G_2$ | Between 0.0 to 6.0 mm | Air gap 2 (between Stator (II) and Piston) |

# CHAPTER 4

# DESIGN REVIEW AND FABRICATION

To realize the new micro air pump design, a prototype must be built. In this Chapter, the process for the fabrication of the first micro pump prototype will be presented. Problems encountered and approaches to solving these problems during the fabrication process will also be presented.

## 4.1 Piston, Inlet Valve Frame and Inlet Valve

The piston includes three parts (as seen in Figure 4.1): (1) main body, (2) inlet valve frame, and (3) inlet valve. The actual fabrication of permanent magnet body was done by Stanford Magnet Inc. in California, and the inlet valve frame was manufactured by Precision Instrument Development Center (PIDC) in Taiwan.

### 4.1.1 Permanent Magnet Piston

The piston made of a permanent magnet is a new concept introduced in this research. The design of this piston is illustrated in Figure 4.1 Literature related to the development or use of such piston has been scant. The permanent magnet magnetic flux generated by the piston will be the major driving force for the pump (the piston itself). To

maximize magnetic flux and to minimize the feature size, the strength of the permanent magnet should be as large as possible. Therefore, the material chosen for the main piston structure was the rare earth magnet (NdFeB, Neodymium-Iron-Boron) due to its high magnetic flux and low cost.

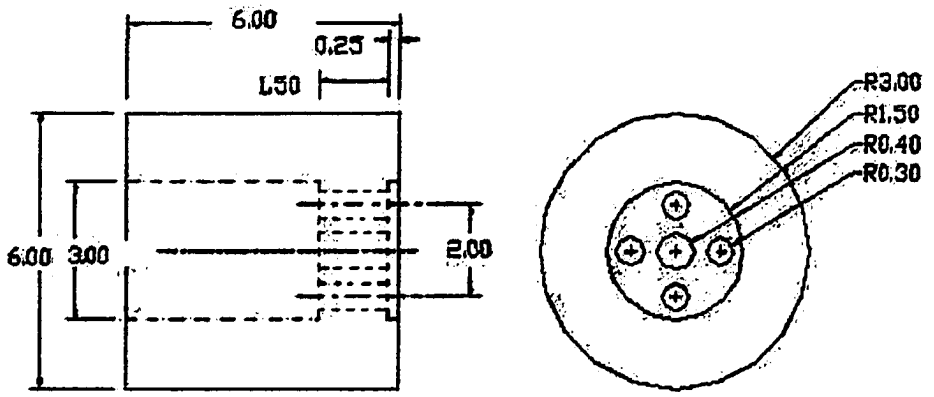


**Figure 4.1 Design of the piston (includes the inlet valve frame)**

NdFeB magnets are higher Maximum Energy Product magnets on today's rare earth magnets market. (BH)max of NdFeB magnets are larger than SmCo magnets, and can easily reach 30 MGOe or even higher, up to 48 MGOe. Actually, the NdFeB magnets have already replaced SmCo magnets in most applications in the last couple of years, especially where the operating temperatures are less than 80 degrees Centigrade. The magnetic performance of NdFeB magnets will deteriorate rapidly when operating at temperatures higher than 180 degrees Centigrade, whereas the SmCo magnets can be operated up to about 250 degrees Centigrade.

There is a trade-off between the magnetic strength and its price; the higher strength the magnet is, the higher the price. Based on the performance calculations

presented in Section 3.3 and considering future production cost, sintered magnets were chosen over bonded magnetic for their better magnetic properties. Since the operating temperature is expected to be lower than 80 degrees Centigrade in this application, the sintered NdFeB (Grade N35) was chosen to be the piston material due to its high magnetic strength, low cast, and availability on the market. The sintered NdFeB permanent magnets are made in several steps.

The following paragraphs are the fabrication processes for the permanent magnet piston from Sanmu Magnets Co., Ltd. First, an NdFeB alloy is formulated based on the properties of the final permanent magnets. In this design, the magnetic flux will be 1.213 Tesla. Details of the permanent magnet materials were not made available due to company policy. The alloy is produced in a vacuum furnace, and then crushed into a powder form. Sintered NdFeB permanent magnets are fabricated using the powder metallurgical process. These magnets can be die pressed or isotropic pressed. During the pressing process, magnetic fields are applied with the help of a specially designed fixture to align magnetic "domains" and optimize the magnetic performance of these magnets (the orientation of the magnetic flux will be along the length of the piston in this design, i.e. the two magnetic poles, south and north will be located at the two end sides of the piston). Then, pressed magnets are placed into a furnace under a protective atmosphere for sintering. After sintering, the magnet shape is rough and needs to be machined and ground in order to achieve the desired shape (cylinder) and size (6.0X3.0X6.0 mm, tolerance: ±0.05 mm for each single data). To protect the magnet and reduce friction, the surface will be coated by a 50μm nickel protective layer. (Additional information about

the permanent magnet piston making processes may be found on Sanmu Magnets Co., Ltd Website.)

### 4.1.2 Inlet Valve Frame

To simplify the fabrication processes, the inlet valve frame and gas holes should be made during the same processes when the permanent magnet piston was made. However, when the prototype was made, there were some problems which make it necessary to make the piston and inlet value frame individually. First of all, the sintered NdFeB magnet is a very fragile and hard material, with good machinability. This means it is almost impossible to drill the inlet valve frame hole and gas holes after the piston is made. Secondly, the inlet valve frame hole (800 μm) and gas holes (600 μm) on the frame were too small for the conventional company to fabricate on the mould before sintering. Therefore, the piston and the inlet valve frame were built individually.

The main purpose of the inlet frame hole is to install the inlet valve on it and let gas through from gas chamber to the outlet. Several different designs have been reviewed and made (see Figure 4.2). Design 1 was chosen in making the prototype for its easy production and assembly. Since the fabrication of the inlet valve frames required the use of micro EDM, assistance was sought from Precision Instrument Development Center (PIDC), Taiwan to make these frames. The following paragraphs describe the fabrication processes for the frames.

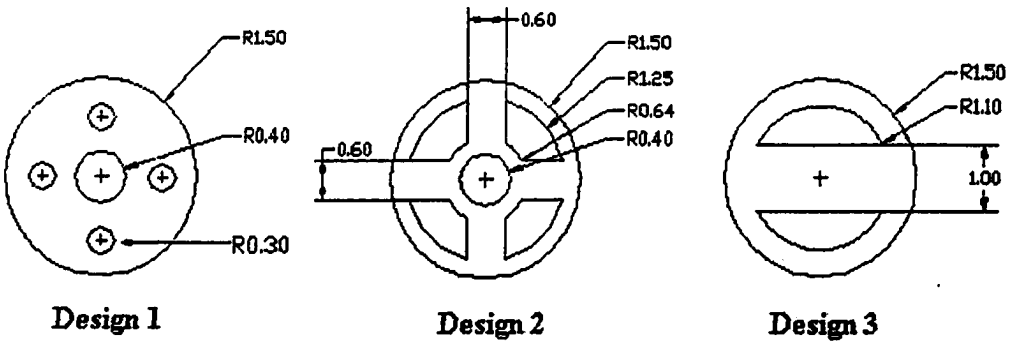


**Figure 4.2 Three different kind of Inlet Valve Frame designs**

The material chosen is A6062 alloy, as it is lighter and softer to mount them together. First, the Charmillies ROBOFIL 2020 Wire EDM (Electrical Discharge Machining) was used to cut the alloy ingot into shape (core, diameter: 3.0 ± 0.05 mm). After the core was made, for the Design 1, the core was cut into the desired length (2.0 ± 0.05 mm). Afterwards, the inlet frame hole (diameter: 0.8 ± 0.05 mm) at the center of the core and 4 gas holes (diameter: 0.6 ± 0.05 mm) were bored around the inlet valve frame hole. For Design 2, after the core was cut into the desired length (2.0 ± 0.05 mm), a taper ring (ID: 2.50 ± 0.05 mm, OD: 3.0 ± 0.05 mm) on a lathe whose internal diameter tightly fitted the shape was bored. The ring was kept on the lathe, and the shape was tightly inserted to the ring. The face was then turned to the same height of the shape, and the part was cut off. A similar procedure for making Design 2 was adopted to make Design 3. The final inlet valve frame is shown in Figure 4.3. (For more details about how Micro EDM work, Charmillie's web site).

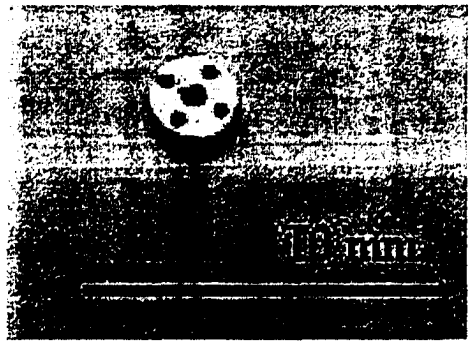

**Figure 4.3 Inlet Valve Frames**

### 4.1.3 Inlet Valve

The inlet valve is a simple structure made by injection rubber (see Figure 4.4). The valve used in this design was directly modified from the valve used on one of the existing commercial micro-air pumps. The diameter was cut from 6.0 mm to 3.0 mm to fit the prototype.

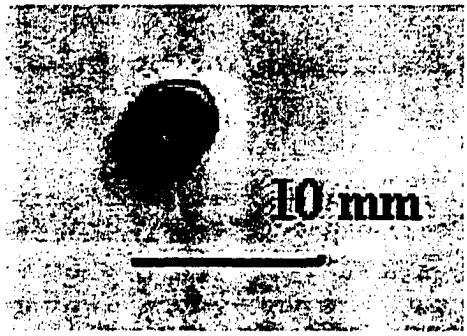


**Figure 4.4 Rubber Inlet Valve**

### 4.1.4 Piston Assembly

After each part had been made, they were assembled together with simple hand tools. Figure 4.5 shows the complete piston assembly.

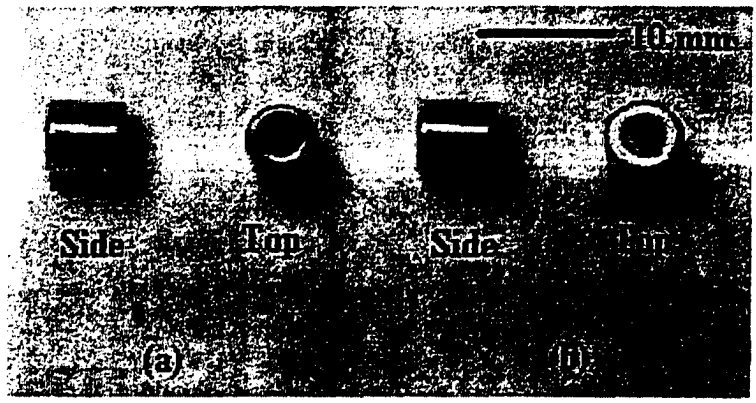


**Figure 4.5 Picture of the Piston (a) without the valve (b) with the valve**

## 4.2 Stators

The electromagnetic forces generated by the stators were the other driving force sources in this design. In order to obtain sufficient driving force, two stators were needed in this design. Two possible designs of the stator locations had been reviewed: (1) to wrap around the piston or (2) to place at the two end sides of the piston. It was decided to place the stators at the two end sides of the piston (see Figure 3.1) after considering the final thickness of the pump and the strength of the magnetic flux interactions between the stators and the piston.

### 4.2.1 Properties of Magnetic Core

The various physical shapes of magnetic core materials can be applied to powdered-iron and ferrite cores as well as to those that are fashioned from steel. The choice between ferrite and powdered iron for the electromagnet core is based on one thing: Saturate ability.

The powdered-iron cores do not saturate easily. Saturation can be defined as $B_s$, which is the maximum value of induction at a specified high value of field strength. After this point, the further increase of intrinsic magnetization with an increase in field strength is minimal. The ferrite cores were easily saturated; thus, they are more suitable for use in circuits such as dc-to-dc converters, magnetic amplifiers, and etc. The ferrite cores have another advantage: the permeability of the ferrite cores is much higher than powdered iron. The permeability of the ferrite could be up to 5000.

If the ferrite cores are so good as descripted above, why are the ferrites cores not used for all applications in which magnetic core material is required? Actually, it's a trade-off between the high permeability and core temperature stability. Generally speaking, the higher permeability a material has, the less stable it will be at higher frequencies. The stability of an inductor is the major factor in critical circuits such as narrow-band filters, narrow-band tuned transformers, and oscillators. If the temperature changed, it might cause the permeability to change, which in some cases can have a marked effect on stability. The higher permeability of the core material has, the more pronounced temperature effect it will have. Therefore, the powdered iron core is often the designer's preference in RF circuits that need to be relatively immune to the effects of saturation and poor stability. Iron core inductors offer high values of Q (quality factor) and stability over a wide range of flux levels and temperature.

### 4.2.2 Design of Magnetic Cores

Based on the design requirements and to get larger electromagnetic forces to drive the piston, the choice of electromagnetic cores in our first version was an iron core, S5-

1802 from Micrometals, Ca. (see Figure 4.6). Unfortunately, there arose another problem: the permanent magnetic force.

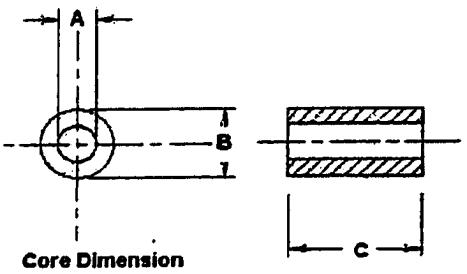


**Figure 4.6 Design for iron and plastic core**

When a ferrous material is placed close to a magnetic object, it will be magnetized by the induced magnetization from the magnetic object. In our design, the iron cores will generate magnetic fields due to the induced magnetization from the piston (permanent magnet). Because of the higher relative permeability of iron cores, the magnetic field interaction (attractive) between those generated from permanent magnets, and induced magnetization in the iron cores will be much larger than the forces (repulsive) between the permanent magnet and electromagnets. Thus, the piston (permanent magnet) will stick on one electromagnet no matter how high the current is applied on the coils (because we do have limitation on the current ampere). This will make the design totally fail.

To resolve the problem of a piston sticking on the iron core, some other nonferrous cores for the electromagnets were re-considered, such as just using a solenoid air core or plastic core (the design as seen in Figure 4.6). Unfortunately, there arose

another problem: the electromagnetic flux/force might become too small for driving the piston under high pressure and long strokes (based on the calculations and simulation results in Chapter 3).

After the failures of the first two designs, a new design using the hybrid core was adopted, which included both ferromagnetic and non-ferromagnetic materials in it for the electromagnetic cores (see Figure 4.7). Based on the electro magnetic theory, when ferromagnetic materials are used in applications such as an iron-core, the relative permeability will provide an idea of the kind of multiplication of the applied magnetic field that can be achieved by having the ferromagnetic core present. So for an ordinary iron core, a magnification of about 2000 might be expected, compared to the magnetic field produced by the solenoid current with just an air or non-ferromagnetic core. At the same time, as the distance (x) between the piston (permanent magnet) and the electromagnetic core became larger, and the strength of magnetic field is based on the order of $1/x^2$, a larger electromagnetic field was achieved and the sticking problem was solved.

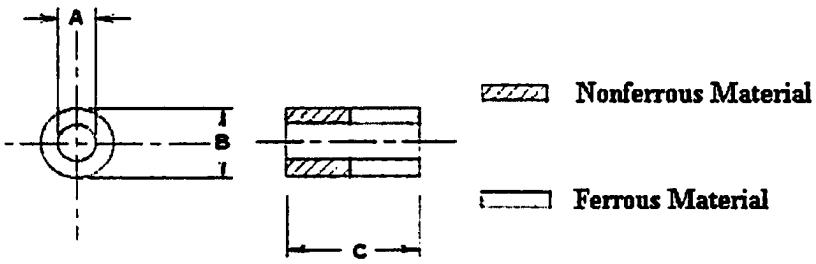


**Figure 4.7 Combination design of the electromagnetic core**

### 4.2.3 Making of Stators

The wire used for the stators is AWG 27, the maximum support for current up to 968mA. The material for ferromagnetic cores is 2673004801 from Fair-Rite Products Corp., NY. For fabricating the stators, 233 turns of wire were wound on each of the hybrid core (see Figure 4.8).

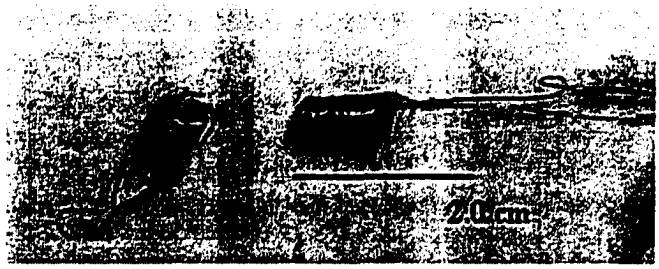

**Figure 4.8 Final product of the Stator**

## 4.3 Cylinder and Gas Chamber

As mentioned earlier, the basic working process of the novel micro pump is like that of a reciprocating pump, which means that there is a piston performing forward and reverse steps in a cylinder to finish the pumping function. Thus, a simple cylinder structure is needed to install the piston. (See Figure 4.9) In a traditional reciprocating pump, there is a need of one input valve and one output valve to control the gas flow moving in just one direction. Since the input valve had already been integrated at the top of the piston, another output valve needed to be built on the gas chamber to allow the gas to move in just one direction.

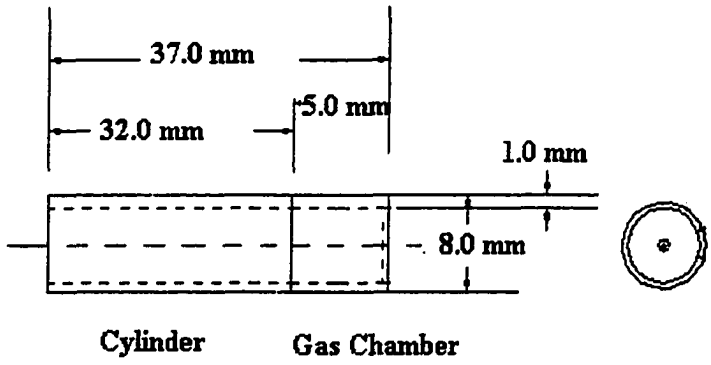


**Figure 4.9 Design and dimension of the cylinder**

For fabricating the cylinder, Teflon from MCMaster was chosen for its great mechanical properties and low friction coefficient (for further details on the Teflon's properties, see Appendix B). The Teflon rod was cut to the required length (32.0 mm). After the rod was cut, in order to obtain a good sealing between the piston and cylinder, a hole was drilled (diameter: 5.95 ± 0.05 mm, just a little bit smaller than the piston) in the center of the rod. Then, it was inserted into the cylinder, and the final cylinder wall treatment was done by hand and sandpaper (Grade: 2000) until the piston just fit in (see Figure 4.10).


**Figure 4.10 Teflon Cylinder**

To simplify the fabrication process, the gas chamber used in this study was directly modified from the one used in P23B-0001-00 -Series micro air pump (from Oken Seiko Co.) as seen in Figure 4.11.

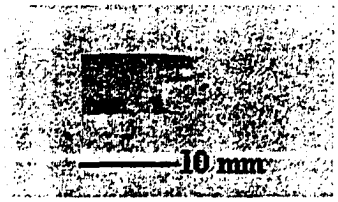


**Figure 4.11 Gas Chamber**

### 4.4 Control Circuit

In order to obtain the input/output processes as the traditional pump does, a control circuit was needed to generate accurate time oscillation to drive/control (frequency and current) the pump.

Normally, the traditional motor/pump structure's motor is driven by a small DC battery, and there exists one or more shafts to change the direction of force in order to obtain the reciprocating motion of the piston and the input and output processes. However, the motor and shaft/shafts would no longer exist in this novel micro pump. Instead, the novel micro pump would be driven directly by magnetic forces. The following paragraphs will discuss the details about how to build the control circuit

Based on design requirements, the power source for this novel pump should be two AAA batteries (3.0 VDC); however, for easy construction and testing, the test version would be based on an LM 555 timer (operation voltage around 4.5 VDC). It was decided to change the oscillation chip from LM 555 timer to ALD 555 timer (operation

voltage is 3.0 VDC) for the final version, so that the install space could be reduced and the design requirements could be matched. Basically, no matter which timer was chosen, the control circuit would include two major parts – the timer for time oscillation and two transistors and a large capacitor for the AC current amplification and generation.

### 4.4.1 Testing Version

The LM 555 timer (see Figure 4.12) is one of the most widely used timers in today's industry. This chip, introduced by Signetics, originally used bipolar ICs. Presently, the LM555 timer chip is available in bipolar or CMOS circuits from various manufacturers. The LM 555 timer could be used in many applications such as precision timing, pulse generation, sequential timing, time delay generation, pulse width modulation, pulse position modulation and linear ramp generator. In this study, the application is in pulse generation and pulse width/position modulation.

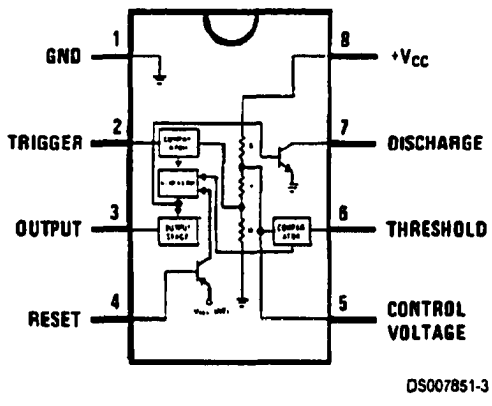


**Figure 4.12 LM555 Timer**

The control circuit, as seen in Figure 4.13, includes two parts – Part A: LM555 timer as oscillator, and Part B: power source, two transistors (NPN, PNP) and a large capacitor for current converting and amplification.

The function of the LM 555 applied in this application is an oscillator. Based on the operation guide, the circuit should be connected as in Figure 4.13 part A. There are three specific points for the duty cycle and frequency control – Resistor A ($R_A$), Resistor B ($R_B$), and Capacitor A (C). The time period ($t_1$) for the output high is

$$t_1 = 0.693 \cdot R_A \cdot C \tag{4.1}$$

The time period ($t_2$) for the output low is

$$t_2 = \left(\left(\frac{R_A \cdot R_B}{R_A + R_B}\right)\right) C \cdot \ln\left(\frac{R_B - 2 \cdot R_A}{2 \cdot R_B - R_A}\right) \tag{4.2}$$

Thus, the frequency (f) of oscillation is

$$f = \frac{1}{t_1 + t_2} \tag{4.3}$$

Based on the data sheet of the LM 555 timer, the circuit will not oscillate if $R_B$ is greater than ½ $R_A$ because the junction of $R_A$ and $R_B$ cannot bring pin 2 down to 1/3 $V_{cc}$ and trigger the lower comparator.

The type of capacitor needed in the design can be found directly from Eq. 4.3. For example, if a 60 Hz with 50% duty cycle oscillator is expected, then $R_A$ and $R_B$ can be set to equal 51KΩ and 22KΩ. By Eq.4.3, a 0.235μF capacitor will be needed to achieve this purpose. More details about the relationship between the resistors and the capacitor on the testing process will be given in the next chapter.

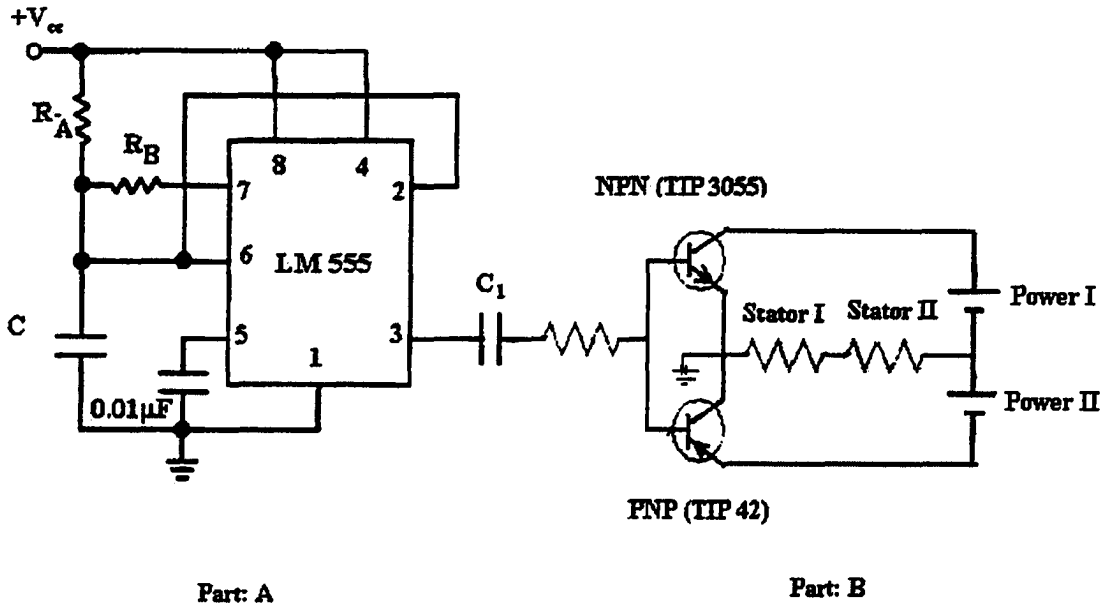


**Figure 4.13 Control Circuit**

The main purpose of the circuit in Figure 4.13 part B is for the AC current amplification and generation. It includes one NPN (TIP 3055, Collector Current up to 10.0A) transistor, one PNP (TIP 42, Collector Current up to 10.0A) transistor, one large capacitor, and one resistor (for the final current adjustment.) (See Figure 4.14)

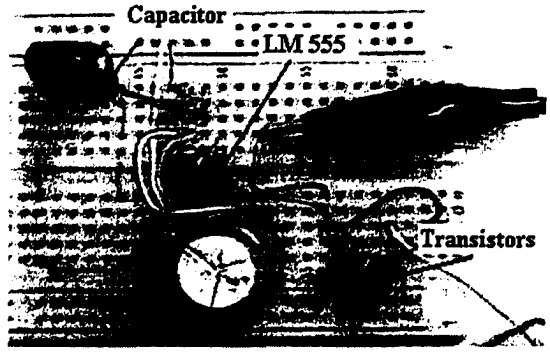


**Figure 4.14 Control circuit (Built on the breadboard)**

### 4.4.2 Final Modified Version for the Company Requirement

Based on the limitation of the LM 555 timer operation voltage and the company requirement (must be operated base on 2 AAA batteries, 3.0 VDC), it was found that another timer that can satisfy the operation situation as the LM 555 was needed. More importantly, it should be operated under 3.0 VDC. ALD555 timer (see Figure 4.15 for chip topography) was the one that was chosen on the final production line.

The ALD555 timer is a high performance monolithic timing circuit built with advanced silicon gate CMOS technology by Advanced Linear Devices, Inc. Basically, the only difference between LM 555 timer and ALD 555 timer is their operation voltage. The ALD555 has all the functions that LM555 had. That means the circuit design based on LM555 could be used directly on an ALD555 base circuit.

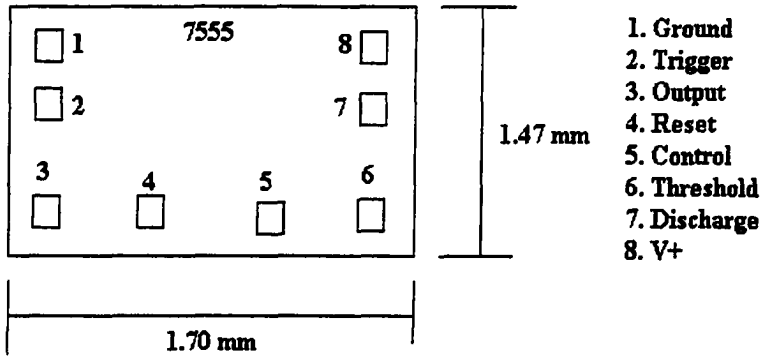


**Figure 4.15 ALD 555 Chip Topography**

Because of the limitations on building such a small feature-size circuit (the chip's dimension is smaller than 2.0 mm) at Tech Lab, and the major purpose of this study is to approve the new design and operation concepts; thus, it didn't need to be built in this paper.

# CHAPTER 5

# FINAL ASSEMBLY AND EXPERIMENT SETUP

## 5.1 Final Assembly

After all the parts had been fabricated as described in Chapter 4, they were assembled together for further testing. Figure 5.1 shows the assembled micro air pump prototype.

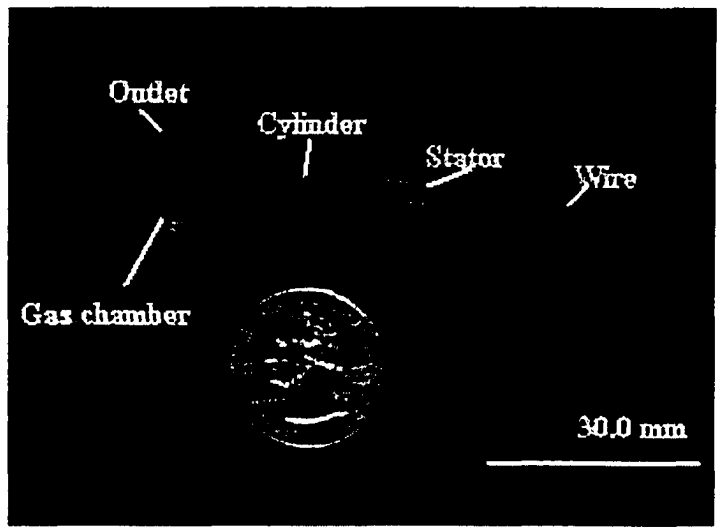


**Figure 5.1 Assembled Micro Air Pump Prototype**

## 5.2 Experiment Setup

The following three pictures show the final experimental setup. For better control and testing of the stroke distance, a stroke distance adjustable table was designed and fabricated, as seen in Figure 5.2. Figure 5.3 shows the final setup of the equipment. Figure 5.4 shows the magnetic flux/field meter used for the permanent magnet and electromagnets magnetic fluxes testing in this study. The meter is a Model 907 Gaussmeter by Magnetic Instrumentation, Inc.

**Figure 5.2 Stroke adjustable table**

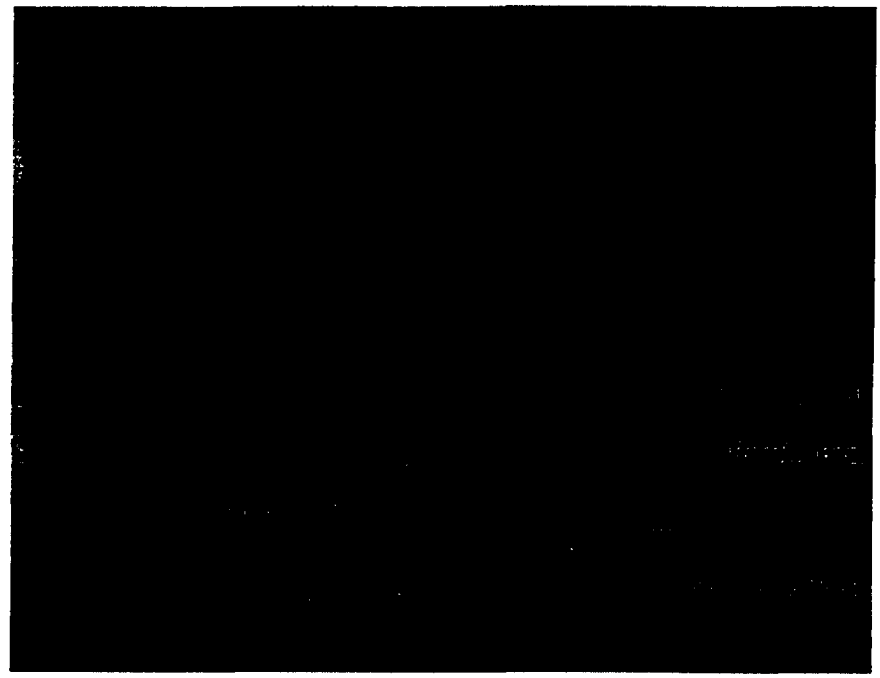

**Figure 5.3 Final equipments setup**

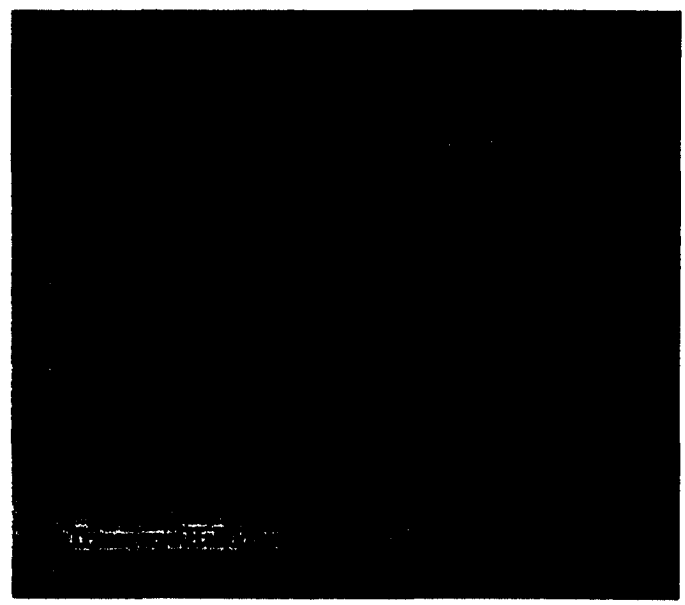

**Figure 5.4 Model 907 GaussMeter**

## 5.3 Results Analysis

### 5.3.1 Experimental Results

Table 5.1 shows the theoretical and test results of the permanent magnet magnetic fluxes strength. One hundred sets of data have been obtained in this study. Partial data of this experiment can be seen in Tables 5.2 to 5.4 and Figures 5.5 to 5.7. The entire data may be found in Appendix B.

**Table 5.1 Permanent magnet magnetic fluxes density theoretical and testing results**

| **Distance from the surface (mm)** | 0.0 | 1.0 | 2.0 | 3.0 | 4.0 | 5.0 | 6.0 |
|---|---|---|---|---|---|---|---|
| **Magnetic Fluxes Density (Theoretical, unit: Gauss)** | 5424 | 3670 | 2333 | 1465 | 960 | 649 | 463 |
| **Magnetic Fluxes Density (Test, unit: Gauss)** | 3667 | 2472 | 1564 | 990 | 642 | 438 | 310 |

**Table 5.2 Results of data set 17**

| Current (A) | E.M.F (Gauss) | Pressure (mmHg) at Stroke = | | | | | |
|---|---|---|---|---|---|---|---|
| | | 1.0 mm | 1.5 mm | 2.0 mm | 2.5 mm | 3.0 mm | 3.5 mm |
| 0.4 | 46 | 10 | -- | -- | -- | -- | -- |
| 0.6 | 74 | 10 | 56 | -- | -- | -- | -- |
| 0.7 | 118 | 10 | 58 | 82 | 110 | -- | -- |
| 0.8 | 179 | 10 | 60 | 84 | 112 | 160 | -- |
| 0.9 | 228 | 10 | 60 | 84 | 114 | 164 | 174 |
| 1.0 | 268 | 12 | 60 | 86 | 114 | 165 | 180 |
| Frequency: 0.22, Sealing (Cylinder): Case III, Inlet Valve Design: Design II | | | | | | | |

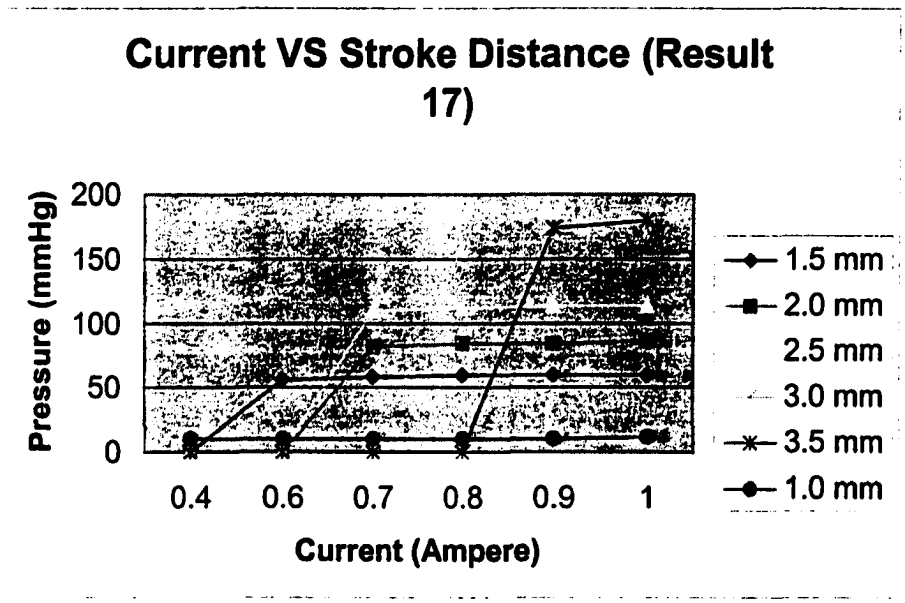


**Figure 5.5 Current VS Stroke Distance (Result 17)**

**Table 5.3 Results of data set 19**

| Current (A) | E.M.F (Gauss) | Pressure (mmHg) at Stroke = | | | | | |
|---|---|---|---|---|---|---|---|
| | | 1.0 mm | 1.5 mm | 2.0 mm | 2.5 mm | 3.0 mm | 3.5 mm |
| 0.4 | 45 | -- | -- | -- | -- | -- | -- |
| 0.6 | 74 | 30 | 58 | -- | -- | -- | -- |
| 0.7 | 128 | 30 | 58 | -- | -- | -- | -- |
| 0.8 | 180 | 30 | 58 | 86 | 100 | 100 | -- |
| 0.9 | 246 | 32 | 60 | 86 | 108 | 104 | -- |
| 1.0 | 284 | 34 | 60 | 90 | 116 | 118 | -- |
| Frequency: 0.247, Sealing (Cylinder): Case III, Inlet Valve Design: Design II | | | | | | | |

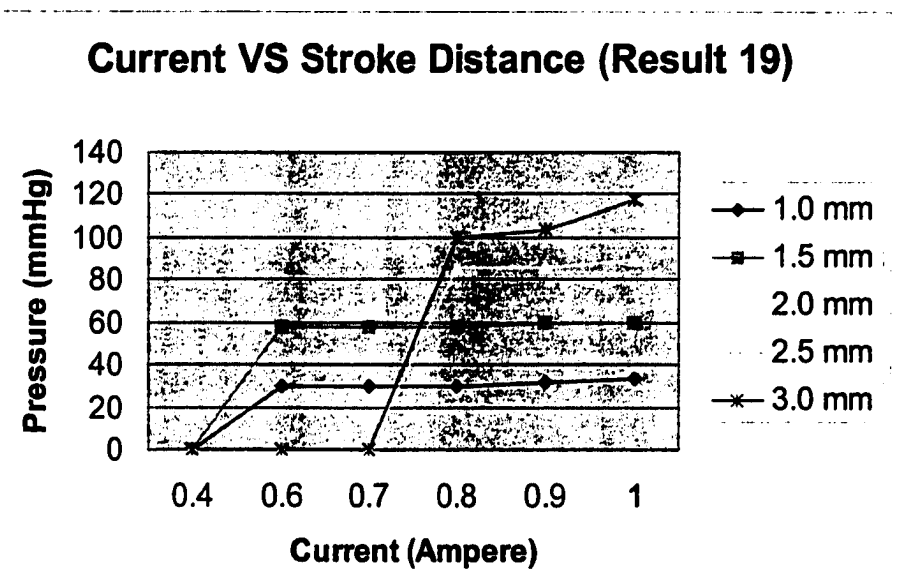


**Figure 5.6 Current VS Stroke Distance (Result 19)**

**Table 5.4 Results of data set 20**

| Current (A) | E.M.F (Gauss) | Pressure (mmHg) at Stroke = | | | | | |
|---|---|---|---|---|---|---|---|
| | | 1.0 mm | 1.5 mm | 2.0 mm | 2.5 mm | 3.0 mm | 3.5 mm |
| **0.4** | **45** | 10 | -- | -- | -- | -- | -- |
| **0.6** | **74** | 28 | 40 | 44 | -- | -- | -- |
| **0.7** | **132** | 29 | 44 | 52 | -- | -- | -- |
| **0.8** | **181** | 30 | 46 | 62 | 60 | -- | -- |
| **0.9** | **233** | 30 | 28 | 70 | 70 | 58 | -- |
| **1.0** | **291** | 32 | 50 | 80 | 78 | 64 | -- |
| Frequency: 0.30, Sealing (Cylinder): Case III, Inlet Valve Design: Design II | | | | | | | |

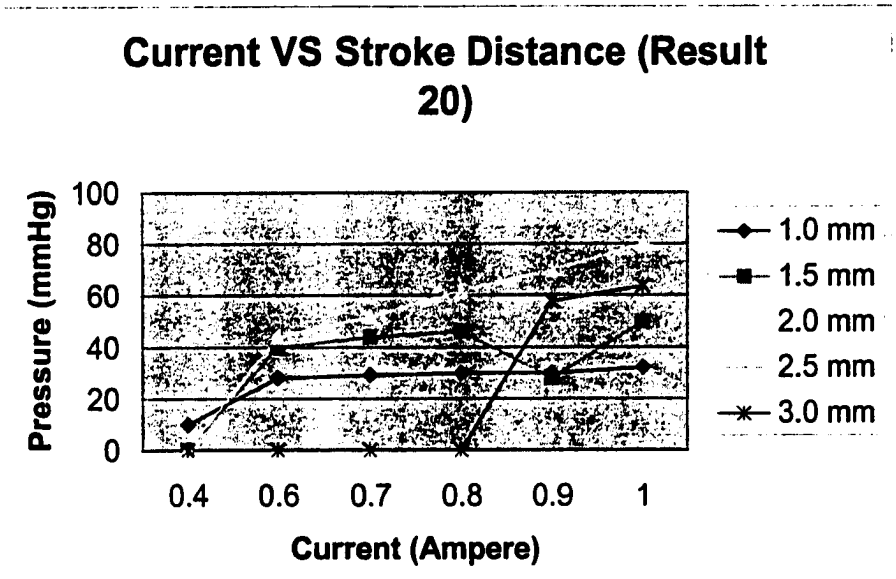


**Figure 5.7 Current VS Stroke Distance (Result 20)**

### 5.3.2 Results Analysis

Based on the theoretical performance calculations and simulation results, this design appears to be able to meet the minimum pressure requirement for use in a blood pressure monitor. However, the experimental results show that the maximum air pressure that this design could attain is 180 mmHg, about 51.5% of the pump used for benchmarking (180 V.S. 350 mmHg). The possible causes for the difference between the theoretical performance calculations and the test results are investigated in the following section, along with possible solutions to this problem.

**Comparisons of Two Designs.** Comparisons between the new design and the existing design are illustrated in Table 5.5

**Table 5.5 Comparisons of Two Designs**

| Item | Original Design | Novel Design |
|---|---|---|
| **The pump size** | 45.0mm X 26.8mm X 12.0mm | 38.0mm X 8.0mm X 8.0mm |
| **Atmosphere** | 20 to 27°C with 30 to 80% RH | 20 to 27°C with 30 to 80% RH |
| **Attitude** | Horizontal | Horizontal |
| **Rated Voltage** | 3.0 V DC | 3.0 V DC |
| **Operating Voltage** | 2.2 to 3.2 V DC | 2.5 to 3.2 V DC |
| **Operating Ampere** | Max 460 mA | Max 900 mA |
| **Pressurizing Time** | Less than 10 sec to pressurize 100 $cm^3$ from 0 to 300 mmHg | 10 sec to pressurize 100 $cm^3$ from 0 to 300 mmHg |
| **Max Noise** | Less than 53dB(A) at 30 cm distance while pressurization | -- |
| **Max Pressure** | More than 350 mmHg at 3.0 V DC | 180 mmHg at 3.0V DC |

## 5.4 Problems

### 5.4.1 Sealing Problem

The most critical factor that affects the performance of an air pump is its sealing ability. A well-sealed air pump is able to achieve the delivered capacity and discharge pressure intended in the design. Good pump sealing, however, can not be attained

without professional craftsmanship and equipment. There are two possible leakage points in the new design: (1) inlet valve V.S. piston and (2) piston V.S. cylinder wall.

**Leakage between inlet valve and piston.** The inlet valve used in this study was modified directly from the current design. The valve was fabricated by hand with simple hand tools and then assembled onto the valve frame manufactured by PIDC. It is apparent that a perfect fit between the inlet vale and the piston does not exist in the new design. This could cause a severe air leakage between the valve and the surface of the piston, leading to substantial pressure drop in the air pumping process. Outsourcing the valve to a professional valve manufacturer may solve this problem.

**Leakage between piston and cylinder wall.** The amount of tolerance allowed between the piston and the cylinder is another factor that determines the degree of air leakage during the pumping process. A small tolerance allows little air to escape but increases the amount of force required to move the piston. On the other hand, a large tolerance reduces the force requirement to move the piston but allows more air to flow through. The trade-off between force requirement and air leakage has been studied in this study.

**Effect of tolerance on pump pressure.** Three different tolerances between the piston and the cylinder wall were tested in this study. The data in Table 5.6 show that the discharge pressure increased exponentially when the piston–cylinder wall tolerance decreased linearly. The discharge pressure changed from 250 Pa (when the piston –

cylinder tolerance was set at 75 μm) to 13.3 KPa (when the piston – cylinder wall distance was set at 25 μm).

**Table 5.6 Effect of piston-cylinder wall tolerances on discharge pressure**

| Piston-Cylinder Wall Distance | 75 μm | 50 μm | 25 μm |
|---|---|---|---|
| **Pressure (Pa)** | 250 | 1998 | 13300 |

*Based on frequency = 120 Hz

To obtain an optimal tolerance that limits air leakage to the minimum level (but still allows smooth movement of piston with minimum amount of force) is a challenging task. To achieve this, the inner wall of the cylinder must be straight and the cylinder surface must be smooth. The cylinder block used in this study was made by a conventional lathe and then ground by hand with a piece of sandpaper (Grade: 2000). It is believed that the roughness of the cylinder wall is high, and the resulting large friction force could hinder the movement of the piston at high frequency. The result could be high air leakage rate and great reduction in the discharge pressure. Potential solutions to this problem include using a high precision lathe for machining the inner wall of the cylinder or using injection technology to make the cylinder.

There was also a wearing away problem facing the Teflon cylinder used in this study. Since the material hardness of the piston (permanent magnet coated by Zn) is much higher than that of the Teflon (cylinder), during the experiments, the cylinder wall was observed to wear away time after time. Consequently, the diameter of the cylinder

grew and the tolerance between the piston and the cylinder increased. This effect was evidenced by the decrease in the pump performances (either delivered capacity or developed pressure) over time during the experiments. One way to solve this problem is to apply a thin coating of Teflon (1 mm) to the surface of the piston to reduce its friction with the cylinder wall.

### 5.4.2 Strength of the Permanent Magnet and Inlet Valve

The strength of the permanent magnet is another problem leading to low discharge pressure. As can be seen in Table 5.1, the test results of the permanent magnet's magnetic flux shown are much smaller than the theoretical values presented in Section 3.3.3.1. Comparisons of these two forces and the pressures reached are list in Table 5.7 below.

**Table 5.7 Comparisons of theoretical and testing results in magnetic flux, force and pressure reached**

| | Magnetic Flux Density | Force Generated | Pressure Reached |
|---|---|---|---|
| **Theoretical** | 5883.914 Gauss | 292110 Dyne | 400 mmHg |
| **Testing** | 3977 Gauss | 133210 Dyne | 180 mmHg |

It's clear that the expected pressure could be reached if the permanent magnet's magnetic flux can reach its theoretical value or a permanent magnet of higher grade is used. There are two reasons that might explain why the permanent magnet magnetic flux

failed to reach its theoretical value: (1) the magnetic circuit efficiency, and (2) the strength of permanent magnetic flux.

To improve the magnetic circuit efficiency, the cylinder may be covered by a layer of magnetic material. This will increase the strength of the magnetic flux inside the cylinder. To improve the permanent magnetic flux strength, one may consider (a) using a higher-grade permanent magnet as the piston material, or (b) reducing the inlet hole diameter of the permanent magnet.

The material used in this study was N35 (Br = 12.13 KGs); thus, if a N45 (Br = 13.50 KGs) or N50 (Br = 14.5 KGs) is used instead, the strength of the magnetic flux will increase by 21%, and this pump will generate a higher discharge pressure. Also, the permanent magnet used in this study has a 3 mm hole in the middle. If the size of the hole is reduced by 1mm, the total volume of the permanent magnet will increase by 26 %, and the strength of the magnetic fluxes will increase by 20%. Again, this will help this design to reach a higher discharge pressure.

### 5.4.3 Solenoid Winding Problem

Winding of the solenoid is done in industry by machines that can spool cooper wire tightly and in good order. The quality of wire winding directly affects the strength of solenoid electromagnet magnetic flux. The wire that formed the solenoid electromagnets used in this study was wound by hand and was not in good order. It is believed that the disordered wire resulted in a reduction of the magnetic flux strength. By using a wire- winding machine to wind the solenoid, the problem could be solved.

### 5.4.4 Diameter of the Air Tube

According to the pressure theory (Pascal law, $P = F_1/A_1=F_2/A_2$), the pressure applied to an enclosed fluid is transmitted undiminished to every point of the fluid and the walls of the containing vessel. That means that the area is a very important factor on pressure effect. In this study, two different sizes of air hole were made and tested (800 μm and 1.10 mm). The result shows that the larger hole was able to reach a higher discharge pressure mainly because the rate of air leakage between the piston and the cylinder wall (when the air hole is large) is smaller than that of a smaller air hole. To force the air through a smaller hole, a large pressure has to be applied. Nevertheless, the large pressure may also cause the air to leak through the space between the piston and the cylinder wall if the sealing is not done properly. To fully understand this problem, an in-depth study on the gas flow profile during the pumping process is necessary.

### 5.4.5 Length Ratio Between the Ferromagnetic and Non-Ferromagnetic Cores in the Combination Core Design

In order to get a higher electromagnetic flux density, the solenoid used in this design is a combination design (half ferromagnetic core and half non-ferromagnetic core.) If the ferromagnetic core is placed too close to the permanent magnet, the interactions between the permanent magnet and ferromagnetic core might be larger than the magnetic flux generated by the electromagnet, causing the piston to stick on the electromagnet. To solve this problem, more studies on the length ratio of these two cores and the ferromagnetic core's relative permeability are needed.

# CHAPTER 6

# CONCLUSIONS AND RECOMMENDATIONS FOR FUTURE RESEARCH

## 6.1 Conclusions

In this research, a novel permanent magnetically and electro-magnetically powered, linear oscillating conventional micro air pump was designed, fabricated and characterized. This pump might be used in a wrist-type blood pressure monitor or other similar devices that require high air pressure discharge. Factors considered in designing this micro air pump include feature size (especially the thickness), operation voltage, efficiency, heat transfer, noise and weight. For evaluating the feasibility of this novel design, basic performance calculations and ANSYS magnetic flux simulations had been conducted before the first prototype was made. Both theoretical calculations and simulation results show that this novel design meets the minimum requirements for use in a wrist-type blood pressure monitor. The developed pump prototype pump was able to achieve a maximum air pressure of 180 mmHg.

### 6.1.1 Advantages

The new micro air pump developed in this research offers the following advantages:

**Size reduction.** Compared to an existing air pump used in a wrist-type blood pressure meter (see Figure 6.1), this new design shows significant reduction in the thickness (reduced by 33%) as well as the overall size (reduced by 50%).

**Noise reduction.** Compared to the existing air pump, the noise generated by the new pump has been reduced due to it brushless design.

**Structure simplification.** The new pump has only one moving part, the piston. It can be easily manufactured at a lower cost than the traditional design.

**Oil-less design.** Lubrication isn't needed in this design, which makes this design maintenance-free after fabricated

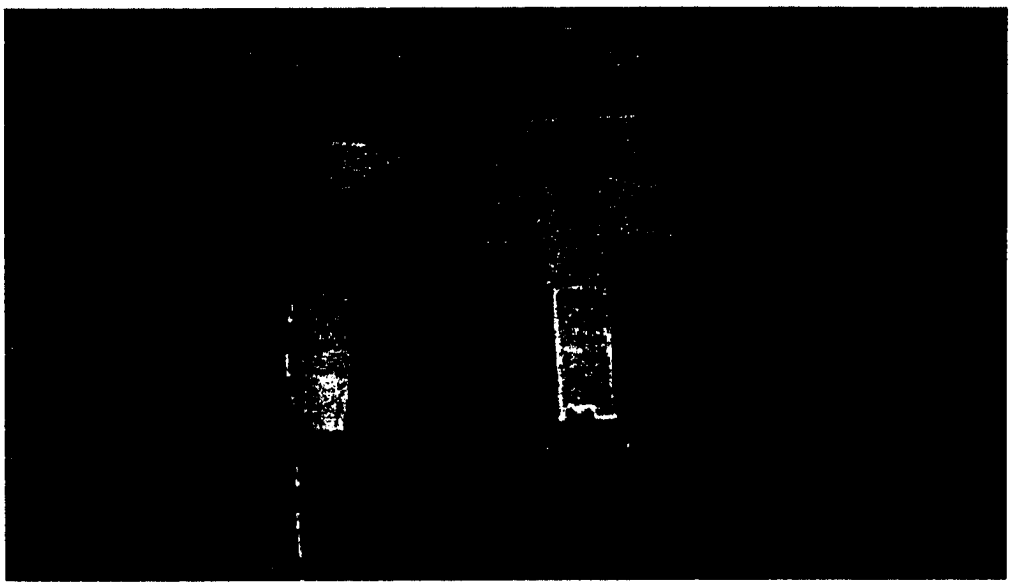

**Figure 6.1 Size Comparisons of the new pump the existing pump**

## 6.2 Recommendations for Future Research

Based on the theoretical performance calculations, ANSYS simulation results, and prototype test data, this new pump design clearly show a great potential to be used in miniaturized devices such as wrist-type blood pressure monitors that require high air pressure discharge. Nevertheless, additional research work will be required before this new pump can be realized commercially. The research tasks recommended for the further improvement of this new pump design are listed below.

(1) Improve the sealing of inlet valve and piston.

(2) Determine the optimal tolerance between the piston and the cylinder wall (i.e., to optimize the gas tube diameter).

(3) Increase the permanent magnet magnetic flux strength.

(4) Optimize the length ratio between the ferromagnetic and non-ferromagnetic cores in the combination core design.

(5) Mechanize the solenoid wire winding process.

# APPENDIX A

# EXCEL RESULTS FOR PERMANENT MAGNET MAGNETIC FLUX DENSITY

| Distance (inch) | | | | Model I | Model II |
|---|---|---|---|---|---|
| 0 | 0.89443 | 0.00000 | 0.97014 | 5424.70091 | -459.21335 |
| 0.001 | 0.89518 | 0.00847 | 0.95344 | 5377.87838 | -404.71189 |
| 0.002 | 0.89593 | 0.01695 | 0.93674 | 5331.02076 | -350.31674 |
| 0.003 | 0.89667 | 0.02542 | 0.92007 | 5284.13968 | -296.10464 |
| 0.004 | 0.89740 | 0.03388 | 0.90345 | 5237.24677 | -242.15162 |
| 0.005 | 0.89812 | 0.04233 | 0.88687 | 5190.35357 | -188.53260 |
| 0.006 | 0.89884 | 0.05078 | 0.87037 | 5143.47161 | -135.32107 |
| 0.007 | 0.89955 | 0.05922 | 0.85395 | 5096.61232 | -82.58875 |
| 0.008 | 0.90025 | 0.06764 | 0.83762 | 5049.78707 | -30.40530 |
| 0.009 | 0.90095 | 0.07605 | 0.82141 | 5003.00712 | 21.16200 |
| 0.01 | 0.90164 | 0.08444 | 0.80531 | 4956.28366 | 72.04854 |
| 0.011 | 0.90232 | 0.09282 | 0.78935 | 4909.62774 | 122.19256 |
| 0.012 | 0.90300 | 0.10117 | 0.77354 | 4863.05030 | 171.53544 |
| 0.013 | 0.90366 | 0.10951 | 0.75788 | 4816.56216 | 220.02185 |
| 0.014 | 0.90433 | 0.11782 | 0.74239 | 4770.17397 | 267.59992 |
| 0.015 | 0.90498 | 0.12610 | 0.72707 | 4723.89626 | 314.22139 |
| 0.016 | 0.90563 | 0.13436 | 0.71194 | 4677.73937 | 359.84168 |
| 0.017 | 0.90627 | 0.14260 | 0.69700 | 4631.71350 | 404.42002 |
| 0.018 | 0.90691 | 0.15080 | 0.68226 | 4585.82863 | 447.91943 |
| 0.019 | 0.90754 | 0.15897 | 0.66773 | 4540.09460 | 490.30679 |
| 0.02 | 0.90817 | 0.16711 | 0.65342 | 4494.52103 | 531.55282 |

| | | | | | |
|---|---|---|---|---|---|
| 0.021 | 0.90879 | 0.17521 | 0.63932 | 4449.11735 | 571.63204 |
| 0.022 | 0.90940 | 0.18328 | 0.62545 | 4403.89276 | 610.52273 |
| 0.023 | 0.91001 | 0.19131 | 0.61181 | 4358.85627 | 648.20685 |
| 0.024 | 0.91061 | 0.19931 | 0.59841 | 4314.01666 | 684.66994 |
| 0.025 | 0.91120 | 0.20726 | 0.58524 | 4269.38248 | 719.90104 |
| 0.026 | 0.91179 | 0.21518 | 0.57231 | 4224.96206 | 753.89251 |
| 0.027 | 0.91238 | 0.22305 | 0.55962 | 4180.76348 | 786.63997 |
| 0.028 | 0.91295 | 0.23088 | 0.54718 | 4136.79459 | 818.14207 |
| 0.029 | 0.91353 | 0.23866 | 0.53498 | 4093.06299 | 848.40041 |
| 0.03 | 0.91409 | 0.24640 | 0.52303 | 4049.57603 | 877.41931 |
| 0.031 | 0.91466 | 0.25409 | 0.51132 | 4006.34083 | 905.20571 |
| 0.032 | 0.91521 | 0.26173 | 0.49985 | 3963.36423 | 931.76895 |
| 0.033 | 0.91577 | 0.26933 | 0.48863 | 3920.65284 | 957.12061 |
| 0.034 | 0.91631 | 0.27687 | 0.47765 | 3878.21300 | 981.27436 |
| 0.035 | 0.91685 | 0.28436 | 0.46691 | 3836.05079 | 1004.24575 |
| 0.036 | 0.91739 | 0.29181 | 0.45641 | 3794.17206 | 1026.05210 |
| 0.037 | 0.91792 | 0.29920 | 0.44615 | 3752.58237 | 1046.71227 |
| 0.038 | 0.91845 | 0.30653 | 0.43612 | 3711.28704 | 1066.24654 |
| 0.039 | 0.91897 | 0.31381 | 0.42632 | 3670.29113 | 1084.67647 |
| 0.04 | 0.91949 | 0.32104 | 0.41675 | 3629.59945 | 1102.02470 |
| 0.041 | 0.92000 | 0.32821 | 0.40740 | 3589.21655 | 1118.31485 |
| 0.042 | 0.92051 | 0.33532 | 0.39828 | 3549.14672 | 1133.57135 |
| 0.043 | 0.92101 | 0.34238 | 0.38938 | 3509.39402 | 1147.81937 |

| | | | | | |
|---|---|---|---|---|---|
| 0.044 | 0.92151 | 0.34938 | 0.38069 | 3469.96225 | 1161.08462 |
| 0.045 | 0.92201 | 0.35632 | 0.37221 | 3430.85496 | 1173.39328 |
| 0.046 | 0.92250 | 0.36321 | 0.36394 | 3392.07547 | 1184.77189 |
| 0.047 | 0.92298 | 0.37003 | 0.35587 | 3353.62685 | 1195.24725 |
| 0.048 | 0.92346 | 0.37680 | 0.34801 | 3315.51194 | 1204.84631 |
| 0.049 | 0.92394 | 0.38350 | 0.34034 | 3277.73335 | 1213.59609 |
| 0.05 | 0.92441 | 0.39015 | 0.33286 | 3240.29345 | 1221.52362 |
| 0.051 | 0.92488 | 0.39673 | 0.32556 | 3203.19439 | 1228.65583 |
| 0.052 | 0.92534 | 0.40326 | 0.31845 | 3166.43813 | 1235.01953 |
| 0.053 | 0.92580 | 0.40972 | 0.31152 | 3130.02636 | 1240.64129 |
| 0.054 | 0.92626 | 0.41612 | 0.30477 | 3093.96061 | 1245.54744 |
| 0.055 | 0.92671 | 0.42246 | 0.29818 | 3058.24217 | 1249.76401 |
| 0.056 | 0.92716 | 0.42874 | 0.29177 | 3022.87214 | 1253.31664 |
| 0.057 | 0.92760 | 0.43496 | 0.28551 | 2987.85144 | 1256.23062 |
| 0.058 | 0.92804 | 0.44112 | 0.27941 | 2953.18077 | 1258.53078 |
| 0.059 | 0.92848 | 0.44721 | 0.27347 | 2918.86067 | 1260.24150 |
| 0.06 | 0.92891 | 0.45325 | 0.26768 | 2884.89148 | 1261.38669 |
| 0.061 | 0.92934 | 0.45922 | 0.26204 | 2851.27338 | 1261.98974 |
| 0.062 | 0.92976 | 0.46513 | 0.25654 | 2818.00637 | 1262.07352 |
| 0.063 | 0.93018 | 0.47098 | 0.25118 | 2785.09028 | 1261.66037 |
| 0.064 | 0.93060 | 0.47676 | 0.24596 | 2752.52479 | 1260.77206 |
| 0.065 | 0.93101 | 0.48249 | 0.24087 | 2720.30943 | 1259.42983 |
| 0.066 | 0.93142 | 0.48815 | 0.23591 | 2688.44358 | 1257.65432 |

| | | | | | |
|---|---|---|---|---|---|
| 0.067 | 0.93183 | 0.49376 | 0.23107 | 2656.92647 | 1255.46563 |
| 0.068 | 0.93223 | 0.49930 | 0.22636 | 2625.75719 | 1252.88326 |
| 0.069 | 0.93263 | 0.50478 | 0.22177 | 2594.93470 | 1249.92616 |
| 0.07 | 0.93303 | 0.51020 | 0.21729 | 2564.45784 | 1246.61269 |
| 0.071 | 0.93342 | 0.51556 | 0.21292 | 2534.32532 | 1242.96065 |
| 0.072 | 0.93381 | 0.52086 | 0.20866 | 2504.53574 | 1238.98727 |
| 0.073 | 0.93420 | 0.52611 | 0.20451 | 2475.08758 | 1234.70922 |
| 0.074 | 0.93458 | 0.53129 | 0.20047 | 2445.97921 | 1230.14263 |
| 0.075 | 0.93496 | 0.53641 | 0.19652 | 2417.20892 | 1225.30306 |
| 0.076 | 0.93534 | 0.54148 | 0.19267 | 2388.77487 | 1220.20557 |
| 0.077 | 0.93571 | 0.54648 | 0.18892 | 2360.67515 | 1214.86465 |
| 0.078 | 0.93608 | 0.55143 | 0.18526 | 2332.90776 | 1209.29430 |
| 0.079 | 0.93645 | 0.55632 | 0.18169 | 2305.47062 | 1203.50801 |
| 0.08 | 0.93682 | 0.56116 | 0.17821 | 2278.36155 | 1197.51877 |
| 0.081 | 0.93718 | 0.56594 | 0.17481 | 2251.57832 | 1191.33907 |
| 0.082 | 0.93754 | 0.57066 | 0.17150 | 2225.11862 | 1184.98094 |
| 0.083 | 0.93789 | 0.57532 | 0.16826 | 2198.98008 | 1178.45596 |
| 0.084 | 0.93824 | 0.57993 | 0.16511 | 2173.16026 | 1171.77525 |
| 0.085 | 0.93859 | 0.58449 | 0.16203 | 2147.65666 | 1164.94946 |
| 0.086 | 0.93894 | 0.58899 | 0.15902 | 2122.46674 | 1157.98887 |
| 0.087 | 0.93928 | 0.59343 | 0.15609 | 2097.58790 | 1150.90330 |
| 0.088 | 0.93962 | 0.59782 | 0.15323 | 2073.01749 | 1143.70219 |
| 0.089 | 0.93996 | 0.60216 | 0.15043 | 2048.75283 | 1136.39458 |

| | | | | | |
|---|---|---|---|---|---|
| 0.09 | 0.94030 | 0.60645 | 0.14770 | 2024.79120 | 1128.98913 |
| 0.091 | 0.94063 | 0.61068 | 0.14503 | 2001.12982 | 1121.49416 |
| 0.092 | 0.94096 | 0.61487 | 0.14243 | 1977.76591 | 1113.91759 |
| 0.093 | 0.94129 | 0.61900 | 0.13989 | 1954.69665 | 1106.26702 |
| 0.094 | 0.94161 | 0.62308 | 0.13741 | 1931.91917 | 1098.54973 |
| 0.095 | 0.94193 | 0.62711 | 0.13498 | 1909.43060 | 1090.77266 |
| 0.096 | 0.94225 | 0.63109 | 0.13261 | 1887.22805 | 1082.94244 |
| 0.097 | 0.94257 | 0.63502 | 0.13030 | 1865.30860 | 1075.06541 |
| 0.098 | 0.94289 | 0.63890 | 0.12803 | 1843.66933 | 1067.14762 |
| 0.099 | 0.94320 | 0.64274 | 0.12582 | 1822.30728 | 1059.19483 |
| 0.1 | 0.94351 | 0.64652 | 0.12366 | 1801.21951 | 1051.21253 |
| 0.101 | 0.94381 | 0.65026 | 0.12155 | 1780.40306 | 1043.20598 |
| 0.102 | 0.94412 | 0.65395 | 0.11948 | 1759.85494 | 1035.18016 |
| 0.103 | 0.94442 | 0.65760 | 0.11747 | 1739.57220 | 1027.13981 |
| 0.104 | 0.94472 | 0.66120 | 0.11549 | 1719.55185 | 1019.08946 |
| 0.105 | 0.94502 | 0.66476 | 0.11356 | 1699.79091 | 1011.03340 |
| 0.106 | 0.94531 | 0.66827 | 0.11168 | 1680.28642 | 1002.97570 |
| 0.107 | 0.94561 | 0.67173 | 0.10983 | 1661.03541 | 994.92026 |
| 0.108 | 0.94590 | 0.67516 | 0.10802 | 1642.03490 | 986.87073 |
| 0.109 | 0.94619 | 0.67854 | 0.10626 | 1623.28193 | 978.83061 |
| 0.11 | 0.94647 | 0.68188 | 0.10453 | 1604.77356 | 970.80320 |
| 0.111 | 0.94676 | 0.68517 | 0.10284 | 1586.50685 | 962.79164 |
| 0.112 | 0.94704 | 0.68843 | 0.10118 | 1568.47885 | 954.79887 |

| | | | | | |
|---|---|---|---|---|---|
| 0.113 | 0.94732 | 0.69164 | 0.09956 | 1550.68666 | 946.82771 |
| 0.114 | 0.94759 | 0.69481 | 0.09798 | 1533.12737 | 938.88078 |
| 0.115 | 0.94787 | 0.69794 | 0.09643 | 1515.79808 | 930.96060 |
| 0.116 | 0.94814 | 0.70104 | 0.09491 | 1498.69592 | 923.06951 |
| 0.117 | 0.94841 | 0.70409 | 0.09342 | 1481.81803 | 915.20973 |
| 0.118 | 0.94868 | 0.70711 | 0.09197 | 1465.16157 | 907.38334 |
| 0.119 | 0.94895 | 0.71008 | 0.09054 | 1448.72372 | 899.59231 |
| 0.12 | 0.94922 | 0.71302 | 0.08914 | 1432.50167 | 891.83847 |
| 0.121 | 0.94948 | 0.71593 | 0.08778 | 1416.49263 | 884.12355 |
| 0.122 | 0.94974 | 0.71879 | 0.08644 | 1400.69385 | 876.44918 |
| 0.123 | 0.95000 | 0.72162 | 0.08513 | 1385.10258 | 868.81685 |
| 0.124 | 0.95026 | 0.72442 | 0.08384 | 1369.71611 | 861.22798 |
| 0.125 | 0.95051 | 0.72717 | 0.08258 | 1354.53172 | 853.68388 |
| 0.126 | 0.95076 | 0.72990 | 0.08135 | 1339.54677 | 846.18579 |
| 0.127 | 0.95101 | 0.73259 | 0.08014 | 1324.75858 | 838.73482 |
| 0.128 | 0.95126 | 0.73524 | 0.07895 | 1310.16454 | 831.33204 |
| 0.129 | 0.95151 | 0.73787 | 0.07779 | 1295.76204 | 823.97842 |
| 0.13 | 0.95176 | 0.74046 | 0.07665 | 1281.54851 | 816.67484 |
| 0.131 | 0.95200 | 0.74301 | 0.07553 | 1267.52140 | 809.42214 |
| 0.132 | 0.95224 | 0.74554 | 0.07444 | 1253.67818 | 802.22106 |
| 0.133 | 0.95248 | 0.74803 | 0.07336 | 1240.01635 | 795.07229 |
| 0.134 | 0.95272 | 0.75049 | 0.07231 | 1226.53344 | 787.97646 |
| 0.135 | 0.95296 | 0.75292 | 0.07128 | 1213.22699 | 780.93413 |

| | | | | | |
|---|---|---|---|---|---|
| 0.136 | 0.95319 | 0.75532 | 0.07026 | 1200.09460 | 773.94580 |
| 0.137 | 0.95343 | 0.75769 | 0.06927 | 1187.13387 | 767.01192 |
| 0.138 | 0.95366 | 0.76003 | 0.06830 | 1174.34242 | 760.13290 |
| 0.139 | 0.95389 | 0.76235 | 0.06734 | 1161.71792 | 753.30909 |
| 0.14 | 0.95412 | 0.76463 | 0.06640 | 1149.25805 | 746.54078 |
| 0.141 | 0.95434 | 0.76688 | 0.06548 | 1136.96053 | 739.82823 |
| 0.142 | 0.95457 | 0.76911 | 0.06458 | 1124.82310 | 733.17166 |
| 0.143 | 0.95479 | 0.77131 | 0.06369 | 1112.84352 | 726.57125 |
| 0.144 | 0.95502 | 0.77348 | 0.06282 | 1101.01959 | 720.02713 |
| 0.145 | 0.95524 | 0.77562 | 0.06196 | 1089.34913 | 713.53940 |
| 0.146 | 0.95545 | 0.77774 | 0.06112 | 1077.82999 | 707.10813 |
| 0.147 | 0.95567 | 0.77983 | 0.06030 | 1066.46004 | 700.73335 |
| 0.148 | 0.95589 | 0.78190 | 0.05949 | 1055.23719 | 694.41506 |
| 0.149 | 0.95610 | 0.78394 | 0.05870 | 1044.15936 | 688.15324 |
| 0.15 | 0.95631 | 0.78595 | 0.05792 | 1033.22451 | 681.94782 |
| 0.151 | 0.95652 | 0.78795 | 0.05715 | 1022.43061 | 675.79874 |
| 0.152 | 0.95673 | 0.78991 | 0.05640 | 1011.77569 | 669.70588 |
| 0.153 | 0.95694 | 0.79185 | 0.05566 | 1001.25776 | 663.66912 |
| 0.154 | 0.95715 | 0.79377 | 0.05494 | 990.87490 | 657.68830 |
| 0.155 | 0.95735 | 0.79567 | 0.05422 | 980.62519 | 651.76325 |
| 0.156 | 0.95756 | 0.79754 | 0.05352 | 970.50673 | 645.89378 |
| 0.157 | 0.95776 | 0.79939 | 0.05283 | 960.51767 | 640.07967 |
| 0.158 | 0.95796 | 0.80122 | 0.05216 | 950.65617 | 634.32071 |

| | | | | | |
|---|---|---|---|---|---|
| 0.159 | 0.95816 | 0.80302 | 0.05149 | 940.92041 | 628.61664 |
| 0.16 | 0.95836 | 0.80480 | 0.05084 | 931.30862 | 622.96721 |
| 0.161 | 0.95855 | 0.80656 | 0.05020 | 921.81901 | 617.37214 |
| 0.162 | 0.95875 | 0.80830 | 0.04957 | 912.44987 | 611.83115 |
| 0.163 | 0.95894 | 0.81002 | 0.04895 | 903.19947 | 606.34393 |
| 0.164 | 0.95914 | 0.81172 | 0.04834 | 894.06612 | 600.91018 |
| 0.165 | 0.95933 | 0.81340 | 0.04774 | 885.04816 | 595.52958 |
| 0.166 | 0.95952 | 0.81506 | 0.04715 | 876.14394 | 590.20178 |
| 0.167 | 0.95971 | 0.81670 | 0.04657 | 867.35184 | 584.92645 |
| 0.168 | 0.95989 | 0.81832 | 0.04600 | 858.67028 | 579.70323 |
| 0.169 | 0.96008 | 0.81992 | 0.04544 | 850.09767 | 574.53178 |
| 0.17 | 0.96026 | 0.82150 | 0.04488 | 841.63246 | 569.41172 |
| 0.171 | 0.96045 | 0.82306 | 0.04434 | 833.27313 | 564.34268 |
| 0.172 | 0.96063 | 0.82460 | 0.04381 | 825.01817 | 559.32428 |
| 0.173 | 0.96081 | 0.82613 | 0.04328 | 816.86610 | 554.35613 |
| 0.174 | 0.96099 | 0.82763 | 0.04277 | 808.81544 | 549.43785 |
| 0.175 | 0.96117 | 0.82912 | 0.04226 | 800.86477 | 544.56904 |
| 0.176 | 0.96135 | 0.83060 | 0.04176 | 793.01266 | 539.74930 |
| 0.177 | 0.96152 | 0.83205 | 0.04127 | 785.25771 | 534.97823 |
| 0.178 | 0.96170 | 0.83349 | 0.04078 | 777.59854 | 530.25542 |
| 0.179 | 0.96187 | 0.83491 | 0.04031 | 770.03379 | 525.58047 |
| 0.18 | 0.96205 | 0.83631 | 0.03984 | 762.56213 | 520.95296 |
| 0.181 | 0.96222 | 0.83770 | 0.03938 | 755.18223 | 516.37247 |

| | | | | | |
|---|---|---|---|---|---|
| 0.182 | 0.96239 | 0.83908 | 0.03892 | 747.89280 | 511.83860 |
| 0.183 | 0.96256 | 0.84043 | 0.03847 | 740.69256 | 507.35092 |
| 0.184 | 0.96273 | 0.84177 | 0.03803 | 733.58024 | 502.90902 |
| 0.185 | 0.96289 | 0.84310 | 0.03760 | 726.55461 | 498.51247 |
| 0.186 | 0.96306 | 0.84441 | 0.03717 | 719.61444 | 494.16086 |
| 0.187 | 0.96322 | 0.84570 | 0.03675 | 712.75852 | 489.85377 |
| 0.188 | 0.96339 | 0.84698 | 0.03634 | 705.98567 | 485.59077 |
| 0.189 | 0.96355 | 0.84825 | 0.03593 | 699.29471 | 481.37145 |
| 0.19 | 0.96371 | 0.84950 | 0.03553 | 692.68451 | 477.19538 |
| 0.191 | 0.96387 | 0.85074 | 0.03513 | 686.15391 | 473.06214 |
| 0.192 | 0.96403 | 0.85196 | 0.03475 | 679.70181 | 468.97133 |
| 0.193 | 0.96419 | 0.85317 | 0.03436 | 673.32710 | 464.92251 |
| 0.194 | 0.96435 | 0.85437 | 0.03398 | 667.02871 | 460.91527 |
| 0.195 | 0.96451 | 0.85555 | 0.03361 | 660.80555 | 456.94920 |
| 0.196 | 0.96466 | 0.85672 | 0.03325 | 654.65659 | 453.02388 |
| 0.197 | 0.96482 | 0.85788 | 0.03288 | 648.58078 | 449.13889 |
| 0.198 | 0.96497 | 0.85902 | 0.03253 | 642.57710 | 445.29384 |
| 0.199 | 0.96512 | 0.86015 | 0.03218 | 636.64455 | 441.48831 |
| 0.2 | 0.96527 | 0.86127 | 0.03183 | 630.78215 | 437.72189 |
| 0.201 | 0.96542 | 0.86238 | 0.03149 | 624.98891 | 433.99417 |
| 0.202 | 0.96557 | 0.86347 | 0.03116 | 619.26387 | 430.30477 |
| 0.203 | 0.96572 | 0.86455 | 0.03082 | 613.60610 | 426.65326 |
| 0.204 | 0.96587 | 0.86562 | 0.03050 | 608.01465 | 423.03927 |

| | | | | | |
|---|---|---|---|---|---|
| 0.205 | 0.96602 | 0.86668 | 0.03018 | 602.48862 | 419.46238 |
| 0.206 | 0.96616 | 0.86772 | 0.02986 | 597.02710 | 415.92221 |
| 0.207 | 0.96631 | 0.86876 | 0.02955 | 591.62920 | 412.41837 |
| 0.208 | 0.96645 | 0.86978 | 0.02924 | 586.29404 | 408.95048 |
| 0.209 | 0.96659 | 0.87080 | 0.02894 | 581.02077 | 405.51813 |
| 0.21 | 0.96674 | 0.87180 | 0.02864 | 575.80853 | 402.12096 |
| 0.211 | 0.96688 | 0.87279 | 0.02834 | 570.65649 | 398.75859 |
| 0.212 | 0.96702 | 0.87377 | 0.02805 | 565.56382 | 395.43064 |
| 0.213 | 0.96716 | 0.87474 | 0.02776 | 560.52970 | 392.13673 |
| 0.214 | 0.96730 | 0.87570 | 0.02748 | 555.55336 | 388.87649 |
| 0.215 | 0.96743 | 0.87665 | 0.02720 | 550.63398 | 385.64957 |
| 0.216 | 0.96757 | 0.87758 | 0.02693 | 545.77081 | 382.45559 |
| 0.217 | 0.96771 | 0.87851 | 0.02666 | 540.96307 | 379.29419 |
| 0.218 | 0.96784 | 0.87943 | 0.02639 | 536.21002 | 376.16503 |
| 0.219 | 0.96798 | 0.88034 | 0.02612 | 531.51091 | 373.06773 |
| 0.22 | 0.96811 | 0.88124 | 0.02586 | 526.86501 | 370.00195 |
| 0.221 | 0.96824 | 0.88213 | 0.02561 | 522.27161 | 366.96735 |
| 0.222 | 0.96838 | 0.88301 | 0.02535 | 517.73000 | 363.96357 |
| 0.223 | 0.96851 | 0.88388 | 0.02510 | 513.23948 | 360.99028 |
| 0.224 | 0.96864 | 0.88475 | 0.02486 | 508.79936 | 358.04714 |
| 0.225 | 0.96877 | 0.88560 | 0.02461 | 504.40898 | 355.13381 |
| 0.226 | 0.96890 | 0.88644 | 0.02437 | 500.06765 | 352.24996 |
| 0.227 | 0.96902 | 0.88728 | 0.02414 | 495.77474 | 349.39527 |

| | | | | | |
|---|---|---|---|---|---|
| 0.228 | 0.96915 | 0.88811 | 0.02390 | 491.52958 | 346.56940 |
| 0.229 | 0.96928 | 0.88893 | 0.02367 | 487.33155 | 343.77204 |
| 0.23 | 0.96940 | 0.88974 | 0.02344 | 483.18002 | 341.00286 |
| 0.231 | 0.96953 | 0.89054 | 0.02322 | 479.07437 | 338.26156 |
| 0.232 | 0.96965 | 0.89133 | 0.02300 | 475.01399 | 335.54781 |
| 0.233 | 0.96978 | 0.89212 | 0.02278 | 470.99828 | 332.86132 |
| 0.234 | 0.96990 | 0.89290 | 0.02256 | 467.02666 | 330.20177 |
| 0.235 | 0.97002 | 0.89367 | 0.02235 | 463.09854 | 327.56886 |

# APPENDIX B

# EXPERIMENT RESULTS

**Result 01**

**Frequency: 0.367**

**Sealing (Cylinder): Case I**

**Inlet Valve Design: Design I**

| Current (A) | E.M.F (Gauss) | Pressure (mmHg) at Stroke = | | | | | |
|---|---|---|---|---|---|---|---|
| | | 1.0 mm | 1.5 mm | 2.0 mm | 2.5 mm | 3.0 mm | 3.5 mm |
| 0.4 | 35 | -- | -- | -- | -- | -- | -- |
| 0.6 | 62 | 5 | -- | -- | -- | -- | -- |
| 0.7 | 85 | 18 | 10 | 5 | -- | -- | -- |
| 0.8 | 121 | 25 | 22 | 15 | 5 | -- | -- |
| 0.9 | 171 | 35 | 30 | 20 | 8 | -- | -- |
| 1.0 | 185 | 44 | 35 | 25 | 13 | -- | -- |

**Result 02**

**Frequency: 0.22**

**Sealing (Cylinder): Case I**

**Inlet Valve Design: Design I**

| Current (A) | E.M.F (Gauss) | Pressure (mmHg) at Stroke = | | | | | |
|---|---|---|---|---|---|---|---|
| | | 1.0 mm | 1.5 mm | 2.0 mm | 2.5 mm | 3.0 mm | 3.5 mm |
| 0.4 | 38 | -- | -- | -- | -- | -- | -- |
| 0.6 | 65 | 5 | -- | -- | -- | -- | -- |
| 0.7 | 85 | 7 | 5 | -- | -- | -- | -- |
| 0.8 | 126 | 22 | 15 | 5 | -- | -- | -- |
| 0.9 | 134 | 36 | 26 | 20 | -- | -- | -- |
| 1.0 | 177 | 58 | 48 | 36 | -- | -- | -- |

**Result 03**

**Frequency: 0.147**

**Sealing (Cylinder): Case I**

**Inlet Valve Design: Design I**

| Current (A) | E.M.F (Gauss) | Pressure (mmHg) at Stroke = | | | | | |
|---|---|---|---|---|---|---|---|
| | | 1.0 mm | 1.5 mm | 2.0 mm | 2.5 mm | 3.0 mm | 3.5 mm |
| 0.4 | 39 | -- | -- | -- | -- | -- | -- |
| 0.6 | 64 | 10 | -- | -- | -- | -- | -- |
| 0.7 | 85 | 18 | -- | -- | -- | -- | -- |
| 0.8 | 104 | 19 | 18 | -- | -- | -- | -- |
| 0.9 | 126 | 42 | 22 | -- | -- | -- | -- |
| 1.0 | 129 | 82 | 28 | -- | -- | -- | -- |

**Result 04**

**Frequency: 0.367**

**Sealing (Cylinder): Case I**

**Inlet Valve Design: Design II**

| Current (A) | E.M.F (Gauss) | Pressure (mmHg) at Stroke = | | | | | |
|---|---|---|---|---|---|---|---|
| | | 1.0 mm | 1.5 mm | 2.0 mm | 2.5 mm | 3.0 mm | 3.5 mm |
| 0.4 | 35 | -- | -- | -- | -- | -- | -- |
| 0.6 | 62 | -- | -- | -- | -- | -- | -- |
| 0.7 | 85 | 28 | 32 | 24 | -- | -- | -- |
| 0.8 | 121 | 30 | 32 | 30 | -- | -- | -- |
| 0.9 | 171 | -- | 38 | 36 | -- | -- | -- |
| 1.0 | 185 | -- | -- | 38 | -- | -- | -- |

**Result 05**

**Frequency: 0.22**

**Sealing (Cylinder): Case I**

**Inlet Valve Design: Design II**

| Current (A) | E.M.F (Gauss) | Pressure (mmHg) at Stroke = | | | | | |
|---|---|---|---|---|---|---|---|
| | | 1.0 mm | 1.5 mm | 2.0 mm | 2.5 mm | 3.0 mm | 3.5 mm |
| 0.4 | 38 | 25 | -- | -- | -- | -- | -- |
| 0.6 | 65 | 28 | -- | -- | -- | -- | -- |
| 0.7 | 85 | 28 | 66 | -- | -- | -- | -- |
| 0.8 | 126 | 28 | 66 | -- | -- | -- | -- |
| 0.9 | 134 | 28 | 66 | 88 | 91 | -- | -- |
| 1.0 | 177 | 28 | 66 | 90 | 106 | -- | -- |

**Result 06**

**Frequency: 0.147**

**Sealing (Cylinder): Case I**

**Inlet Valve Design: Design II**

| Current (A) | E.M.F (Gauss) | Pressure (mmHg) at Stroke = | | | | | |
|---|---|---|---|---|---|---|---|
| | | 1.0 mm | 1.5 mm | 2.0 mm | 2.5 mm | 3.0 mm | 3.5 mm |
| 0.4 | 39 | -- | -- | -- | -- | -- | -- |
| 0.6 | 64 | 5 | 2 | -- | -- | -- | -- |
| 0.7 | 85 | 10 | 5 | -- | -- | -- | -- |
| 0.8 | 104 | 14 | 30 | -- | -- | -- | -- |
| 0.9 | 126 | 15 | 42 | -- | -- | -- | -- |
| 1.0 | 129 | 22 | 42 | -- | -- | -- | -- |

**Result 07**

**Frequency: 0.367**

**Sealing (Cylinder): Case II**

**Inlet Valve Design: Design I**

| Current (A) | E.M.F (Gauss) | Pressure (mmHg) at Stroke = | | | | | |
|---|---|---|---|---|---|---|---|
| | | 1.0 mm | 1.5 mm | 2.0 mm | 2.5 mm | 3.0 mm | 3.5 mm |
| 0.4 | 22 | -- | -- | -- | -- | -- | -- |
| 0.6 | 39 | -- | -- | -- | -- | -- | -- |
| 0.7 | 54 | -- | -- | -- | -- | -- | -- |
| 0.8 | 80 | -- | -- | -- | -- | -- | -- |
| 0.9 | 96 | 10 | 10 | -- | -- | -- | -- |
| 1.0 | 120 | 10 | 20 | 18 | -- | -- | -- |

**Result 08**

**Frequency: 0.22**

**Sealing (Cylinder): Case II**

**Inlet Valve Design: Design I**

| Current (A) | E.M.F (Gauss) | Pressure (mmHg) at Stroke = | | | | | |
|---|---|---|---|---|---|---|---|
| | | 1.0 mm | 1.5 mm | 2.0 mm | 2.5 mm | 3.0 mm | 3.5 mm |
| 0.4 | 24 | -- | -- | -- | -- | -- | -- |
| 0.6 | 37 | -- | -- | -- | -- | -- | -- |
| 0.7 | 54 | -- | -- | -- | -- | -- | -- |
| 0.8 | 67 | -- | -- | -- | -- | -- | -- |
| 0.9 | 87 | 10 | 8 | 4 | -- | -- | -- |
| 1.0 | 101 | 10 | 10 | 5 | -- | -- | -- |

**Result 09**

**Frequency: 0.147**

**Sealing (Cylinder): Case II**

**Inlet Valve Design: Design I**

| Current (A) | E.M.F (Gauss) | Pressure (mmHg) at Stroke = | | | | | |
|---|---|---|---|---|---|---|---|
| | | 1.0 mm | 1.5 mm | 2.0 mm | 2.5 mm | 3.0 mm | 3.5 mm |
| 0.4 | 39 | -- | -- | -- | -- | -- | -- |
| 0.6 | 47 | -- | -- | -- | -- | -- | -- |
| 0.7 | 54 | -- | -- | -- | -- | -- | -- |
| 0.8 | 63 | -- | -- | -- | -- | -- | -- |
| 0.9 | 79 | 10 | 4 | 4 | -- | -- | -- |
| 1.0 | 82 | 18 | 8 | 8 | -- | -- | -- |

**Result 10**

**Frequency: 0.367**

**Sealing (Cylinder): Case II**

**Inlet Valve Design: Design II**

| Current (A) | E.M.F (Gauss) | Pressure (mmHg) at Stroke = | | | | | |
|---|---|---|---|---|---|---|---|
| | | 1.0 mm | 1.5 mm | 2.0 mm | 2.5 mm | 3.0 mm | 3.5 mm |
| 0.4 | 22 | -- | -- | -- | -- | -- | -- |
| 0.6 | 39 | -- | -- | -- | -- | -- | -- |
| 0.7 | 54 | -- | -- | -- | -- | -- | -- |
| 0.8 | 80 | 2 | 10 | 22 | -- | -- | -- |
| 0.9 | 96 | 4 | 16 | 24 | -- | -- | -- |
| 1.0 | 120 | 5 | 18 | 25 | -- | -- | -- |

**Result 11**

**Frequency: 0.22**

**Sealing (Cylinder): Case II**

**Inlet Valve Design: Design II**

| Current (A) | E.M.F (Gauss) | Pressure (mmHg) at Stroke = | | | | | |
|---|---|---|---|---|---|---|---|
| | | 1.0 mm | 1.5 mm | 2.0 mm | 2.5 mm | 3.0 mm | 3.5 mm |
| 0.4 | 24 | -- | -- | -- | -- | -- | -- |
| 0.6 | 37 | -- | -- | -- | -- | -- | -- |
| 0.7 | 54 | -- | -- | -- | -- | -- | -- |
| 0.8 | 67 | -- | -- | -- | -- | -- | -- |
| 0.9 | 87 | -- | -- | -- | -- | -- | -- |
| 1.0 | 101 | -- | -- | 2 | -- | -- | -- |

**Result 12**

**Frequency: 0.147**

**Sealing (Cylinder): Case II**

**Inlet Valve Design: Design II**

| Current (A) | E.M.F (Gauss) | Pressure (mmHg) at Stroke = | | | | | |
|---|---|---|---|---|---|---|---|
| | | 1.0 mm | 1.5 mm | 2.0 mm | 2.5 mm | 3.0 mm | 3.5 mm |
| 0.4 | 39 | -- | -- | -- | -- | -- | -- |
| 0.6 | 47 | -- | -- | -- | -- | -- | -- |
| 0.7 | 54 | -- | -- | -- | -- | -- | -- |
| 0.8 | 63 | -- | -- | -- | -- | -- | -- |
| 0.9 | 79 | 4 | 2 | -- | -- | -- | -- |
| 1.0 | 82 | 5 | 2 | -- | -- | -- | -- |

**Result 13**

**Frequency: 0.367**

**Sealing (Cylinder): Case III**

**Inlet Valve Design: Design I**

| Current (A) | E.M.F (Gauss) | Pressure (mmHg) at Stroke = | | | | | |
|---|---|---|---|---|---|---|---|
| | | 1.0 mm | 1.5 mm | 2.0 mm | 2.5 mm | 3.0 mm | 3.5 mm |
| 0.4 | 44 | 2 | -- | -- | -- | -- | -- |
| 0.6 | 74 | 4 | -- | -- | -- | -- | -- |
| 0.7 | 141 | 16 | 10 | 8 | -- | -- | -- |
| 0.8 | 187 | 18 | 12 | 10 | -- | -- | -- |
| 0.9 | 268 | 21 | 18 | 14 | -- | -- | -- |
| 1.0 | 303 | 24 | 19 | 16 | -- | -- | -- |

**Result 14**

**Frequency: 0.22**

**Sealing (Cylinder): Case III**

**Inlet Valve Design: Design I**

| Current (A) | E.M.F (Gauss) | Pressure (mmHg) at Stroke = | | | | | |
|---|---|---|---|---|---|---|---|
| | | 1.0 mm | 1.5 mm | 2.0 mm | 2.5 mm | 3.0 mm | 3.5 mm |
| 0.4 | 46 | -- | -- | -- | -- | -- | -- |
| 0.6 | 74 | 8 | 4 | -- | -- | -- | -- |
| 0.7 | 118 | 20 | 10 | 6 | -- | -- | -- |
| 0.8 | 179 | 24 | 18 | 10 | -- | -- | -- |
| 0.9 | 228 | 28 | 20 | 16 | -- | -- | -- |
| 1.0 | 268 | 31 | 22 | 18 | -- | -- | -- |

**Result 15**

**Frequency: 0.147**

**Sealing (Cylinder): Case III**

**Inlet Valve Design: Design I**

| Current (A) | E.M.F (Gauss) | Pressure (mmHg) at Stroke = | | | | | |
|---|---|---|---|---|---|---|---|
| | | 1.0 mm | 1.5 mm | 2.0 mm | 2.5 mm | 3.0 mm | 3.5 mm |
| 0.4 | 46 | -- | -- | -- | -- | -- | -- |
| 0.6 | 74 | 24 | 12 | 8 | -- | -- | -- |
| 0.7 | 101 | 30 | 26 | 18 | -- | -- | -- |
| 0.8 | 136 | 32 | 30 | 22 | -- | -- | -- |
| 0.9 | 163 | 34 | 32 | 24 | -- | -- | -- |
| 1.0 | 197 | 38 | 36 | 28 | -- | -- | -- |

**Result 16**

**Frequency: 0.367**

**Sealing (Cylinder): Case III**

**Inlet Valve Design: Design II**

| Current (A) | E.M.F (Gauss) | Pressure (mmHg) at Stroke = | | | | | |
|---|---|---|---|---|---|---|---|
| | | 1.0 mm | 1.5 mm | 2.0 mm | 2.5 mm | 3.0 mm | 3.5 mm |
| 0.4 | 44 | 4 | 2 | 0 | -- | -- | -- |
| 0.6 | 74 | 25 | 24 | 10 | -- | -- | -- |
| 0.7 | 141 | 27 | 30 | 24 | -- | -- | -- |
| 0.8 | 187 | 28 | 40 | 26 | -- | -- | -- |
| 0.9 | 268 | 30 | 42 | 46 | -- | -- | -- |
| 1.0 | 303 | 31 | 50 | 52 | -- | -- | -- |

**Result 17**

**Frequency: 0.22**

**Sealing (Cylinder): Case III**

**Inlet Valve Design: Design II**

| Current (A) | E.M.F (Gauss) | Pressure (mmHg) at Stroke = | | | | | |
|---|---|---|---|---|---|---|---|
| | | 1.0 mm | 1.5 mm | 2.0 mm | 2.5 mm | 3.0 mm | 3.5 mm |
| 0.4 | 46 | 10 | -- | -- | -- | -- | -- |
| 0.6 | 74 | 10 | 56 | -- | -- | -- | -- |
| 0.7 | 118 | 10 | 58 | 82 | 110 | -- | -- |
| 0.8 | 179 | 10 | 60 | 84 | 112 | 160 | -- |
| 0.9 | 228 | 10 | 60 | 84 | 114 | 164 | 174 |
| 1.0 | 268 | 12 | 60 | 86 | 114 | 165 | 180 |

**Result 18**

**Frequency: 0.147**

**Sealing (Cylinder): Case III**

**Inlet Valve Design: Design II**

| Current (A) | E.M.F (Gauss) | Pressure (mmHg) at Stroke = | | | | | |
|---|---|---|---|---|---|---|---|
| | | 1.0 mm | 1.5 mm | 2.0 mm | 2.5 mm | 3.0 mm | 3.5 mm |
| 0.4 | 46 | 20 | -- | -- | -- | -- | -- |
| 0.6 | 74 | 38 | 30 | 20 | -- | -- | -- |
| 0.7 | 101 | 40 | 38 | 24 | -- | -- | -- |
| 0.8 | 136 | 40 | 44 | 26 | -- | -- | -- |
| 0.9 | 163 | 40 | 50 | 30 | -- | -- | -- |
| 1.0 | 197 | 40 | 52 | 32 | -- | -- | -- |

# REFERENCES


[01] F. M. White, *Fluid Mechanics*. New York: McGraw-Hill, 1986.

[02] Anders Olsson, *Valve-less Diffuser Micropumps,* degree of Doctor of Philosophy dissertation, Royal Institute of Technology, 1998

[03] Igor J. Karassik, William C. Krutzsch, Warren H. Faraser, Joseph P. Messina, *Pump Handbook*. New York: McGraw-Hill, 1976. 1-1 ~ 1-4

[04] DEPCO Pump Company, *Pump catalog 205*, 2002 2-4, 41-42

[05] Raymond A. Serway, *Physics For Scientists And Engineers With Modern Physics*, CBS COLLAGE PUBLISHING, 1983 402-662

[06] *http://hyperphysics.phy-astr.gsu.edu/hbase/magnetic/magfor.html#c2* 2002

[07] Magnet Formulas, *http://www.geocities.com/CapeCanaveral/Hall/6153* 2002

[08] Earl M. Underhill, *Permanent Magnet Handbook*, Crucible Steel Company of America, 1957 2-32 ~ 2-36

[09] Rollin J. Parker, *Advances In Permanent Magnetism*, A Wiley-Interscience Publication, 1990 186-218

[10] Daldor Motion Products, *Servo, Linear & Motion Control Products*, 2002 J-1~J-29

[11] Raymond Ramshaw, R. G. van Heeswijk, *Energy Conversion Electric Motors And Generators*, Saunders Collage Publishing, 1990 234-237

[12] Andrew Stubbs. "*Modeling and controller design of an electromagnetic engine valve* ", degree thesis, University of Illinois at Urbana-Champaign, 2000

[13] Chun Tai, Tsu-Chin Tsao, "Quiet seating control design of an electromagnetic engine valve actuator", Proceedings of 2001 ASME International Mechanical Engineering Congress and Exposition, Nov 11-16, 2001 New York, NY

[14] Sanford D. Delong, "*Electromagnetic reciprocating pump and motor means*" US Patent 4692673, Sep 1987

[15] Advances Motion Technologies, "*Electromagnetic valve for bodily fluid drainage*", http://www.q3000.com/products-servoram.asp#docs 2002

[16] PumpWorks Inc. "Dual solenoid pump technology", http://www.pumpworks-inc.com/technology.cfm 2001

[17] Motohashi, Ryo Tanahashi, Masao Amaya, Hidetoshi Maekawa, Takio Okamoto, Toyokatsu Ibuki, Yasuo Oudet, Claude Prudham, Daniel, " *Linear oscillating motor*" US Patent 5736796, Apr 1998

[18] MiniBooster Hydraulics A/S, "*Products Manual*" http://www.minibooster.com/ 2001

[19] Eastern Nishikigoi, "*Medo air pump*" http://www.enkoi.com/pumps/medo.html 2002

[20] Dr. Blood Pressure Online, "*How To Measure The Blood Pressure*" http://www.drbloodpressure.com/05-mesurer.shtml Apr 2002

[21] Sensidyne, Inc. "*Product Manual*", http://www.sensidyne.com/oem/oemAAA.htm 2002

[22] Hargraves Technology Corporation, www.hartechcorp.com/btc_series_pumps.htm

[23] KNF Neuberger Inc., http://www.knf.com/usa.htm 2002

[24] Thomas Pumps & Compressors, http://www.thomaspumps.com 2002

[25] OKEN SEIKO CO. LTC product P23B-0001 manual, Apr 10 1997

[26] P. Gravesen, J. Brandebjerg, and O. Søndergard Jensen, "*Microfluidics - a review*," Journal of Micromechanics and Microengineering, vol. 3 (1993) 168-182

[27] V. Gass, B.H. van der schoot, S. Jeannert and N.F. de. Rooij "*Integrated flow-regulated silicon micropump*" Sensor and Actuators A, 43 (1994) 335-338

[28] Ahn, Chong H; Allen, Mark G. "*Fluid micropumps based on rotary magnetic actuators*" Proceedings of IEEE Micro Mechanical Systems Proceeding of the 1995 IEEE Micro Electro Mechanical Systems Conference Jan 29-Feb 2, 1995 Amsterdam, 408-412

[29] Maillefer, Didier, Van Lintel, Harald "*High-performance silicon micropump for an implantable drug delivery system*". IEEE 1999 12th conference Fl, 541-546

[30] Zengerle, R; Ulrich, J: "*Bidirectional silicon micropumps*" Sensors and Actuators, V50n1-2 Aug 1995 81-86

[31] Rasmussen, Angela; Zaghoul, Mona E "*Pumping techniques available for use in biomedical analysis system*" IEEE 1999 42nd Aug 08-11 1999v2 1999 Las Cruces 656-659

[32] Thomas Weisener, Gerald Vogele, Mark Widmann, Carlo Bark, Rolf Dieter Schraft "*Development and fabrication of a rotary micropump and its industrial and medical applications*". 218 SPIE Vol. 2882

[33] Ansgar Wego and Lienhard Pagel, "*A self-filling micropump based on PCB technology*", Sensors and Actuators A: Physical (88) March 2001 220-226

[34] Cleopatra Cabuz, William R. Herb, Eugen I. Cabuz, Son Thai Lu, "*The dual diaphragm pump*", V 7803, IEEE Jan 2001, 519-522

[35] R Agrawal, Q Hasan, N Ashraf, K B Sundram, L C Chow, J S Kapat and J Vaidya, " *Design and fabrication of meso-scale variable capacitance motor for miniature heat pumps*" Journal of Micromechanics and Microengineering, 13 2003, 1-7

[36] S. Shoji and M. Esashi, "*Microflow devices and systems*," Journal of Micromechanics and Microengineering, vol. 4 (1994) 157-171

[37] J. G. Smits, "*Piezoelectric Micropump with Three Valves Working Peristaltically*," *Sensors and Actuators*, vol. A21-A23 (1990) 203-206

[38] H. T. G. van Lintel, F. C. M. van den Pol, and S. Bouwstra, "*A piezoelectric micropump based on micromachining in silicon*," Sensors and Actuators, vol. 15 (1988) 153-167.

[39] R. Zengerle, S. Kluge, M. Richter, and A. Richter, "*A Bidirectional Silicon Micropump*," IEEE 8th International Workshop on Micro Electro Mechanical Systems (MEMS'95), Amsterdam, the Netherlands, Jan. 29 - Feb. 2, 1995 19-24

[40] E. Stemme and G. Stemme, "*A Valve-less Diffuser/Nozzle based Fluid Pump,*" Sensors and Actuators, vol. A39 (1993) 159-167.

[41] C. H. Ahn and M. G. Allen, "*Fluid Micropumps Based on Rotary Magnetic Actuators*," IEEE 8th International Workshop on Micro Electro Mechanical Systems (MEMS'95), Amsterdam, the Netherlands, Jan. 29-Feb. 2, 1995, 408-412

[42] Sanmu Magnets Co., Ltd. www.sanmumagnets.com 2001

[43] R.D. Cook, D. S. Malkus, and M. E. Plesha, *Concepts and applications of finite element analysis, third ed.* New York: John Wiley & Sons, 1989

[44] ANSYS MultiPhysics Operation Manual, *Basic Analysis Procedures*, 2001

[45] ANSYS MultiPhysics Operation Manual, *Electromagnetic Field Analysis Guide*, 2001

[46] Kirk Biegler, "Material testing systems optimized by the use of moving magnet linear motors", Endura TEC Systems Corporation, www.enduratec.com, 2002

[47] Lipkens, B., D. Perkins and LeLande, F. "*Introduction to Acoustic Compressors*" ASME IMCE. 2000

[48] Baldassare DiBartolo, *Classical Theory Of Electromagnetism*, Prentice Hall, Englewood Cliffs, New Jersey, 1991

[49] Jianming Jin, *Electromagnetic Analysis And Design In Magnetic Resonance Imaging*, Boca Raton London, New York Washington, D.C. 1999

[50] Thomas A. DeMassa, *Electrical and Electronic Devices, Circuit and Instruments*, West Publishing Company, 1989

[51] Plant Design and Experiment, p530~539]

[52] http://www.hartechcorp.com/btc_series_pumps.htm

[53] P. Gravesen, J. Brandebjerg, and O. Søndergard Jensen, "Microfluidics - a review," *Journal of Micromechanics and Microengineering*, vol. 3 (1993) 168-182.

[54] S. Shoji and M. Esashi, "Microflow devices and systems," *Journal of Micromechanics and Microengineering*, vol. 4 (1994) 157-171.

[55] J. G. Smits, "Piezoelectric Micropump with Three Valves Working Peristaltically," *Sensors and Actuators*, vol. A21-A23 (1990) 203-206.

[56] H. T. G. van Lintel, F. C. M. van den Pol, and S. Bouwstra, "A piezoelectric micropump based on micromachining in silicon," *Sensors and Actuators*, vol. 15 (1988) 153-167.

[57] R. Zengerle, S. Kluge, M. Richter, and A. Richter, "A Bidirectional Silicon Micropump," IEEE 8th International Workshop on Micro Electro Mechanical Systems (MEMS'95), Amsterdam, the Netherlands, Jan. 29 - Feb. 2, 1995, pp. 19-24.

[58] E. Stemme and G. Stemme, "A Valve-less Diffuser/Nozzle based Fluid Pump," *Sensors and Actuators*, vol. A39 (1993) 159-167.

[59] C. H. Ahn and M. G. Allen, "Fluid Micropumps Based on Rotary Magnetic Actuators," IEEE 8th International Workshop on Micro Electro Mechanical Systems (MEMS'95), Amsterdam, the Netherlands, Jan. 29-Feb. 2, 1995, pp. 408-412.

[60] Erich Becker *Mechanically Driven Diaphragm Pumps For Use With Gases* Vulkan-Verlag Publishers, Essen Germany 1999, pp.

[61] R.D. Cook, D. S. Malkus, and M. E. Plesha, Concepts and applications of finite element analysis, third ed. New York: John Wiley & Sons, 1989